International
Progress Report

IPR-02-08

Äspö Hard Rock Laboratory

U/Th Isotopes as Natural Analogues for the Mobility of Actinides in Granitic Rocks

Kurt Mengel
Antje Gerdes

Technische Universität Clausthal
Institut für Mineralogie und Mineralische Rohstoffe
Fachgebiet Mineralogie-Geochemie-Salzlagerstätten

November 2001

Svensk Kärnbränslehantering AB
Swedish Nuclear Fuel
and Waste Management Co
Box 5864
SE-102 40 Stockholm Sweden
Tel 08-459 84 00
+46 8 459 84 00
Fax 08-661 57 19
+46 8 661 57 19

Äspö Hard Rock
Laboratory

Report no.
IPR-02-08
No.
F58.2
Author
Kurt Mengel,
Antje Gerdes
Date
Nov. 2001
Checked by
Date

Approved
Christer Svemar
Date
2004-03-09

Äspö Hard Rock Laboratory

U/Th Isotopes as Natural Analogues for the Mobility of Actinides in Granitic Rocks

Kurt Mengel
Antje Gerdes

Technische Universität Clausthal
Institut für Mineralogie und Mineralische Rohstoffe
Fachgebiet Mineralogie-Geochemie-Salzlagerstätten

November 2001

Keywords: Uranium, thorium, natural analogues, actinide mobility

Abstract

The short-lived decay products of ^{238}U (^{234}U and ^{230}Th) can be used as natural analogues for actinides in a hard rock repository. Their mobility in the past may serve as a key for understanding actinide migration in the future. Within the granitoids of the HRL Äspö and of the FL Grimsel, secondary minerals (carbonates, silicates) occur as fracture-fillings which are at least one million years old. Some of the calcite-dominated fracture minerals of the HRL Äspö, however, may also be of a more recent origin. In the older fracture minerals of the HRL Äspö and the FL Grimsel, U is fixed in low concentrations (usually <10 ppm) and it is assumed to have been in or close to the state of secular equilibrium with its short-lived daughters. Upon reaction of the fracture minerals with migrating underground solutions the activity ratios of $^{234}U/^{238}U$ and $^{230}Th/^{234}U$ significantly deviate from unity. The deviation of these activity ratios from unity is a measure of the time elapsed since the event of isotope disturbance, *i.e.* the specific separation of ^{234}U from ^{238}U and of ^{234}U from ^{230}Th by reaction of migrating fluids with fracture filling material.

A total of 18 fracture minerals from the HRL Äspö and 14 fracture minerals from the FL Grimsel have been investigated for their U/Th isotope ratios by therm-ion mass spectrometry (TIMS). From these isotope dilution analyses, the activity ratios of $^{234}U/^{238}U$ and $^{230}Th/^{234}U$ were calculated and found to be out of secular equilibrium. To interpret these data in terms of the age and the degree of disturbance a number of different cases had to be considered. These include the specific gain or loss of ^{234}U relative to ^{238}U and ^{230}Th from an older (≥ 1 Ma) preexisting state of secular equilibrium and the formation of new calcites from solutions carrying $^{234}U/^{238}U$ activity ratios > 1. In the latter case the age of formation can directly be read from the measured activity ratios if the initial $^{234}U/^{238}U$ activity ratios are known.

For the model of preexisting calcites of the HRL Äspö the age of disturbance ranges from 30 to 436 thousand years (ky) at degrees of disturbance ranging from 0.5 to 6.7. If a model of primary (i.e. without preexisting precursors) formation of calcite is assumed, the age of formation ranges from 16 to 275 ky. However, the identification of primary calcite formation in individual fracture fillings is very difficult. The vast majority of mineral assemblages found in healed fractures is certainly of old (> 1 Ma) origin. Thus, the model of isotopic disturbance of preexisting calcite is much more likely for the HRL Äspö. The results obtained for this model imply that during the past 440 ky U was mobile throughout the tunnel sections investigated. Within this section there is a spatial relation between *i)* the age and the degree of disturbance and *ii)* the position of samples from a central axis of an assumed volume of water/rock interaction.

For the FL Grimsel the interpretation of $^{234}U/^{238}U$ and $^{230}Th/^{234}U$ activity ratios within these complex calcite-silicate assemblages is more complicated. Here, a model of open system reactions has to be involved where calcite is dissolved and new calcite is formed within a single fracture while the silicate material has partially lost ^{234}U. Beside the partial gain and loss of ^{234}U, a solid/solid reaction has to be considered where U and Th have been mobilized on a mm scale by α-recoil-induced reaction. Since these reactions have taken place in open systems, neither their age nor their degree of isotopic disturbance can be calculated. However, the disequilibrium states of $^{234}U/^{238}U$ and

$^{230}Th/^{234}U$ activity ratios implies that the reactions causing isotopic disturbances have occurred within the past 500 ky. Only for a set of four calcite-dominated fracture fillings are two mixing events postulated which have occurred between 8 and 80 ky before present. Unlike the results obtained for the HRL Äspö, there is no spatial correlation of $^{234}U/^{238}U$ and $^{230}Th/^{234}U$ activity ratios and the position of fractures containing secondary minerals.

The U/Th-isotope data of both the samples from the HRL Äspö and the FL Grimsel have in common the mobilization of U by migrating solutions within the past 500 ky. As for the question of a final disposal of radioactive waste in granite host rocks, the transport of at least uranium - and thus of the similarly behaving actinides - in migrating underground solutions can therefore not be ruled out.

The current study may serve as a first step towards further investigation of U/Th isotopic equilibria in a more extended volume of Äspö granitoids in that it presents a set of examples for exploiting the spatial and temporal information which are fixed in fracture minerals. In addition, the present study has worked out the methodical principles of interpreting complex U/Th isotope signatures for the short-lived daughters down to ^{230}Th which may serve as tools for further projects dealing with U/Th isotopes as natural analogues for actinide migration in fracture systems of granitic rocks.

Contents

1 Introduction and objectives

1.1 U/Th-decay series as a natural analogue

The quality of the geological barrier and the behaviour of migrating fluids within it play an important role in assessing the safety of silicate hard rocks for the final disposal of high-active waste. In this respect, research into the mobility of actinides is of particular interest. It is very difficult, however, to use elements from radioactive waste as tracers in field experiments to study their migration. Our proposal, therefore, is that the migration behaviour of natural analogues such as U and Th should be investigated.

The natural-occurring elements U and Th have large ionic radii and high ion charges. This is why their mobility behaviour in granitic rocks qualifies them as an analogue of transuranium elements. U is relatively soluble as a carbonate complex $\{(UO_2(CO_3)_3)^{4-}\}$ and can be transported in aqueous solutions without difficulty. It is fixed in $CaCO_3$ when it precipitates. In comparison, Th is virtually immobile. On the basis of the isotope distribution of short-lived decay products (half-life: $^{234}U = 2.5 \cdot 10^5$ a; $^{230}Th = 7.5 \cdot 10^4$ a) in new formations of secondary fracture fillings, the date of a possible migration of U in solutions in granitic rock can be determined for a period of between 5 ky and 400 ky in the past with the help of fracture fillings formed from migrating solutions. The information carried by the U/Th-isotope system answers the question whether these two elements have been mobilized in the granitic rock in the past 400 ky or have stayed there undisturbed. In the latter case, one can assume an analogous behaviour in the next 400 ky.

1.2 General aims of the project

The general aim of the project has been to give an account of the mobility of U along both its spatial and temporal dimensions within the geological barrier granite. The relevant question at the root of this approach is whether natural-occurring uranium has been mobilized in the past 400 ky. If this is not the case, one can predict from a geoscientist's perspective with a reasonable degree of probability that this will not happen in the coming 400 ky either. If the state of secular disequilibrium in the fracture fillings shows, however, that U has been mobilized to a considerable extent, it is to be expected by analogy that U and possibly transuranium elements will be transported in solutions in the future, as well. While the research project 02E 8916 (April 1996 to October 1999) focused on the spreading of those elements that occur in high-active waste, the present study pursues a different approach: to infer from the behaviour of U and Th the potential migration of actinides and to emphasize the temporal classification of U migration.

1.3 Specific aims of the project

1. *Selection of fracture fillings in the granitic complexes of the HRL Äspö and the FL Grimsel which are suitable with respect to their U- and Th-contents*. The original plan to collect half of the samples in the HRL Äspö tunnel failed because suitable sections were difficult to access for sampling. The other half of the samples were to come from drill cores, but in the FL Grimsel samples contained an insufficient amount of the necessary fracture fillings. Therefore, 26 samples were taken from drill cores in the HRL Äspö, and 20 fracture fillings were collected in the tunnel of the FL Grimsel. Subsequently, these samples were chemically examined by means of ICP-MS to determine their chemical composition and their natural U- and Th-contents.
2. *Examination of the U/Th-isotope system in fracture fillings in joints and geological fault zones for disturbed or undisturbed secular equilibria*. The absolute concentration of all three isotopes was analyzed by the isotope dilution-technique employing suitable spikes. The isotope abundances derived from isotope dilution mass spectrometry were converted into activities of ^{238}U, ^{234}U, and ^{230}Th. These activities show whether ^{238}U is in a secular equilibrium with the two sequential isotopes ^{234}U and ^{230}Th.
2. *Integrating U-mobility into the fluid migration systems of the two granitic substances with special emphasis on the temporal dimension*. In the case of the HRL Äspö at least the recent hydraulic context and the origin of the mixing components of underground solutions are known. Some recently formed carbonates in principal can be related to the hydrogeochemically characterized mixtures of *deep saline water*, *modified baltic sea water*, etc. (see e.g. LAAKSOHARJU and WALLIN, 1995) according to their occurrence. This does not hold for the older secondary fracture fillings; they do not show a connection with the current hydraulic system, since it has already been altered through tunneling and drilling. These carbonates must have originated from older solutions within the granite. If, for example, a carbonate vein was formed 500 ky ago, it can be expected to show secular equilibrium for the U- and Th-isotopes in a closed system. If, on the other hand, older fracture fillings have come into contact with HCO_3-bearing solutions of more recent underground solutions, one can date the superimposition on the basis of the deviation from the U/Th secular equilibrium. This is the approach for the secondary fracture fillings of the FL Grimsel, which largely lack a discernible connection with current underground solution systems.
4. *Interpretation of the natural analogue U/Th-isotopes in granites from the HRL Äspö and the FL Grimsel*. The data on the U-Th-isotope distribution of fracture fillings in granites obtained here were used to develop models of the mobility of U and Th in silicate hard rock formations. This included a comparison of the states of the secular equilibrium/disequilibrium of the different fracture filling generations, with particular consideration of the different hydrothermal and hydrous water/rock interactions that took place in the HRL Äspö and the FL Grimsel.

1.4 Organizational context of the research project

Since 1983, the BMWi has supported research on granitic rock formations within a scheme funding R+D-programs for the final disposal of radioactive waste to gain or deepen knowledge on other potential host rock formations beyond investigations confined to ‘rock salt’ as a geological host rock. Work of this type has been in progress in cooperation with the NAGRA in the *Felslabor* (FL) Grimsel since 1983, and with SKB in the Hard-Rock-Laboratory (HRL) Äspö since 1995.

The present study is a contribution to current research on granitic rocks as suitable repositories. Its aim is to aid the assessment of the mobility of actinides using as examples the elements U and Th. Within the BMWi-funding scheme it is related to the research area A4.4E (Characterization and assessment of potential host rock formations), and in particular to the projects B5.2-E (Investigation of geological processes with respect to migration, natural analogues). There is a further link to B7.3-E (Investigation of natural analogues with respect to the long-term behaviour and long-term safety of repositories).

2 Principles of U/Th isotope series dating and equilibria

2.1 Geochemistry and mobilization processes

Both the elements uranium and thorium belong to the actinide group and have similar electron configurations and ionic radii (U^{4+} = 0.89 Å, Th^{4+} = 0.94 Å, MARSHALL and FAIRBRIDGE, 1999). The differences in the geochemical behaviour of these elements, e.g. during the magmatic differentiation, can therefore be considered marginal. According to GASCOYNE (1992) uranium and thorium are more likely to be found in late-stage crystallizing magma, granite and pegmatite, for example, because of their large ionic radii and the resulting high incompatibility. The worldwide uniform Th/U-mass ratio in crustal rocks is 3.5 (WEDEPOHL, 1995); CHERDYNSTEV (1971) gives an average of 4.3 for granites.

Unlike the quadrivalent Th, U can proceed to an oxidation stage 6^+ under oxidizing conditions, e.g. in the process of the surface-water-dominated weathering of rocks. A result of this most stable form are soluble uranyl complex ions (UO_2^{2+}), which, according to DICKIN (1995), have a long average residence time of more than 300 ky in natural waters, the average residence time of thorium is 350 years. Further complex formation (LANGMUIR, 1978) depends on the pH-value and the presence of additional ions.

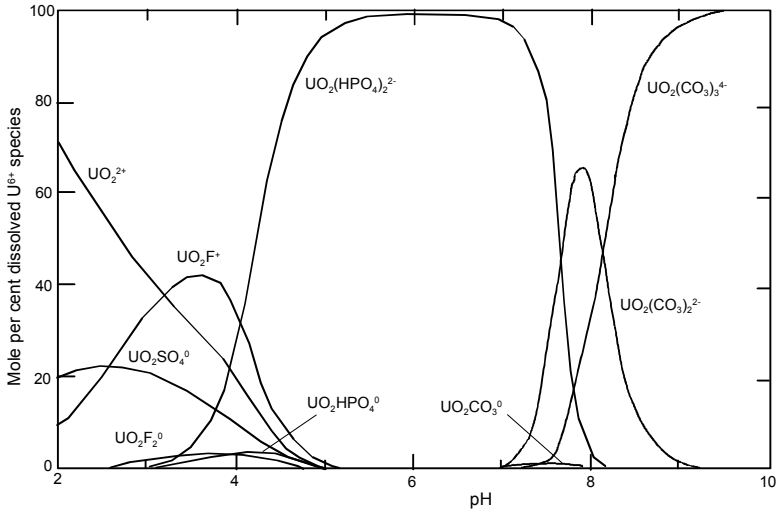

Fig.2.1: *Uranyl-complexes as a function of pH at 25°C in the presence of additional ions (in ppm): ΣF=0.3, ΣCl=10, ΣSO_4=100, ΣPO_4=0.1, ΣSiO_2=30 (after LANGMUIR, 1978).*

Fig. 2.1. indicates that in the case of low U^{6+}-concentration and a pH-value <2.5 the fluorine anion is the dominant complex, followed by the sulfate complex with pH = 2.5 –3, the phosphate complex with pH = 3- 7.5, and the carbonate complex with pH >7.5. If fracture fillings are predominantly carbonates, one can assume a pH-value > 7.5 in the solution flowing through the rock.

2.2 Isotope geochemistry and age-determination

Uranium has three natural-occurring radioactive isotopes: ^{238}U, ^{235}U and ^{234}U. The natural occurrence of thorium, on the other hand, is almost exclusively restricted to the isotope ^{232}Th. The relative abundance, decay constants and half-lives of the most important isotopes for age-determination are presented in Fig. 2.2:

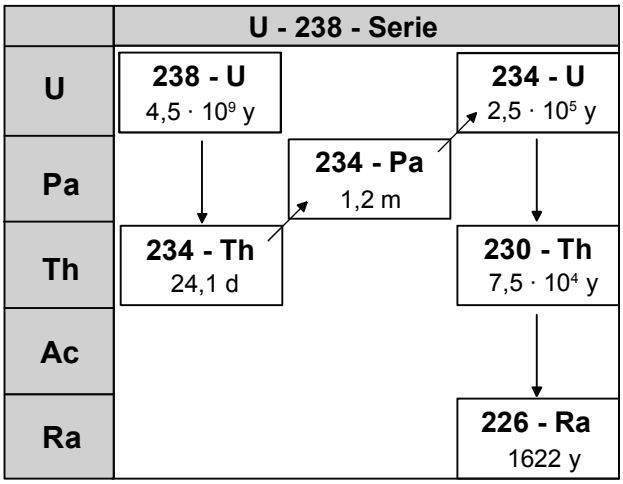

Fig. 2.2: *Naturally occurring radionuclides being used in geological age determination (according to OSMOND und COWART, 1982)*

Dating on the basis of the U-decay series differs from some other methods in that the daughter nuclides produced by the decay are radioactive as well. If a U-bearing system remains undisturbed over a period of > one million years, a secular equilibrium emerges, which means that the activities of the mother and daughter isotopes within a given decay series are identical.

The abundance of each nuclide is proportional to its half-life and inversely proportional to its decay constant. The fact that every system tends to restore the secular equilibrium after a disturbance and that this decay is proportional to time is exploited for dating. Starting from the observation that the decay constant λ is constant for each isotope, Eq. 2.1 is defined:

$$-\frac{dn}{dt} = \lambda n \qquad \text{(Eq. 2.1)}$$

The expression (dn/dt) represents the change of still existing atoms in time and thus the atoms still available for the decay process. The value is a negative one since it gradually decreases in time. If we now integrate the following transposed form

$$\frac{dn}{n} = -\lambda dt \qquad \text{(Eq. 2.2)}$$

over the entire time of decay (from t=0 to t), with n_0 representing the number of atoms n at t=0, we arrive at the radioactive decay law in the form of Eq. 2.5:

$$\int_{n_0}^{n} \frac{dn}{n} = -\lambda \int_{t=0}^{t} dt \qquad \text{(Eq. 2.3)}$$

$$\ln \frac{n}{n_0} = -\lambda t \qquad \text{(Eq. 2.4)}$$

$$n = n_0 \cdot e^{-\lambda t} \qquad \text{(Eq. 2.5)}$$

In this form, the decay law is expressed in terms of the number of atoms, but by means of the following relation

$$\text{Activity}\,(A) = \frac{\text{number of atoms (n)}}{\text{decay constant (l)}} \qquad \text{(Eq. 2.6)}$$

it can also be defined through activities:

$$A = A_0 \cdot e^{-\lambda t}. \qquad \text{(Eq. 2.7)}$$

Using activity-ratios, Eq. 2.7 takes the following form for the example $^{234}U/^{238}U$:

$$\frac{A(^{234}U)}{A(^{238}U)} = \left[\frac{A(^{234}U)}{A(^{238}U)}\right]_0 \cdot e^{-\lambda_{234} t} \qquad \text{(Eq. 2.8)}$$

A uniform value for the $^{234}U/^{238}U$ activity-ratio of 1.14 ±0.02 in recent sea waters can be observed worldwide (e.g. CHEN et al. 1986). This is a reference value for sea water and is therefore also valid for carbonates of marine origin in their initial state. Assuming this initial ratio, the evolution of the activity ratios $^{234}U/^{238}U$, $^{230}Th/^{234}U$, and $^{230}Th/^{238}U$ is represented in Fig. 2.3.

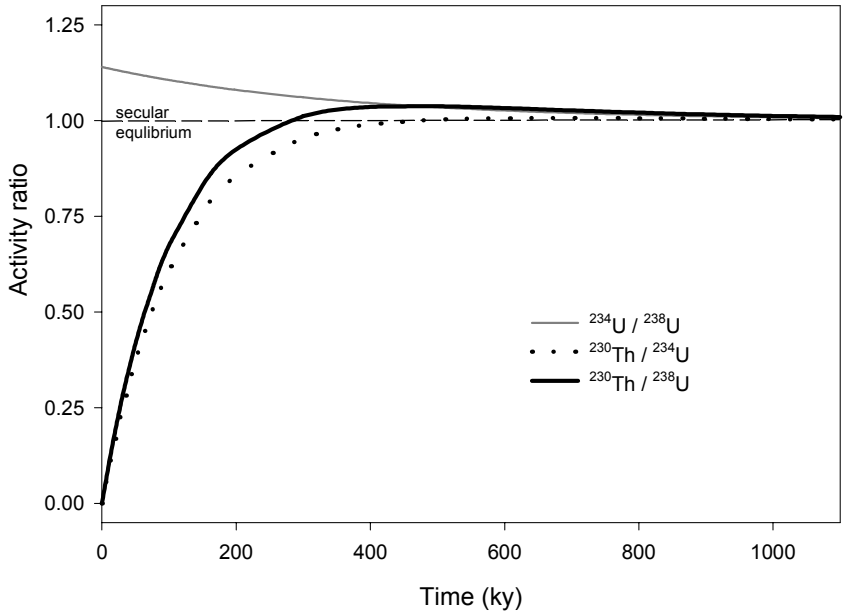

Fig. 2.3: *Evolution of $^{234}U/^{238}U$, $^{230}Th/^{234}U$ and $^{230}Th/^{238}U$ activity ratios for calcites formed from modern sea water starting at an initial $^{234}U/^{238}U$ activity ratio of 1.14 .*

The decay of ^{238}U to ^{234}U occurs via an intermediate stage of two short-lived daughter products. Since the two isotopes are chemically identical, one would think that they are not fractionated in geological processes. Contrary to expectations the final daughter product is slightly enriched, however. The explanation for this process is that the daughter isotope ^{234}U recoils from its lattice position in a given mineral due to the α-decay of its mother and is less firmly fixed in the mineral as a result ('alpha-recoil-effect'). According to OSMOND and COWART (1982) the energy set free in the decay process is strong enough to dislocate the daughter isotope by several Å. If uranium is transported into sea water, e.g. through weathering of continental crust, it is ^{234}U that is predominantly scoured out from the rock and released into the sea water. If the environment has a pH-value higher than 7.5, the stable uranyl carbonate complex is formed. In the case of the precipitation of calcium carbonate from sea water, e.g. in corals, the $^{234}U/^{238}U$- activity ratio of 1.14 is 'frozen' as a value technically known as the initial value of the sample. If the system remains undisturbed over a longer period of time, a secular equilibrium emerges as a result, since the fast-decaying ^{234}U decreases in comparison with ^{238}U. The current $^{234}U/^{238}U$- activity ratio makes it possible to determine the age e.g. of corals due to its proportionality to the past time (Fig. 2.4).

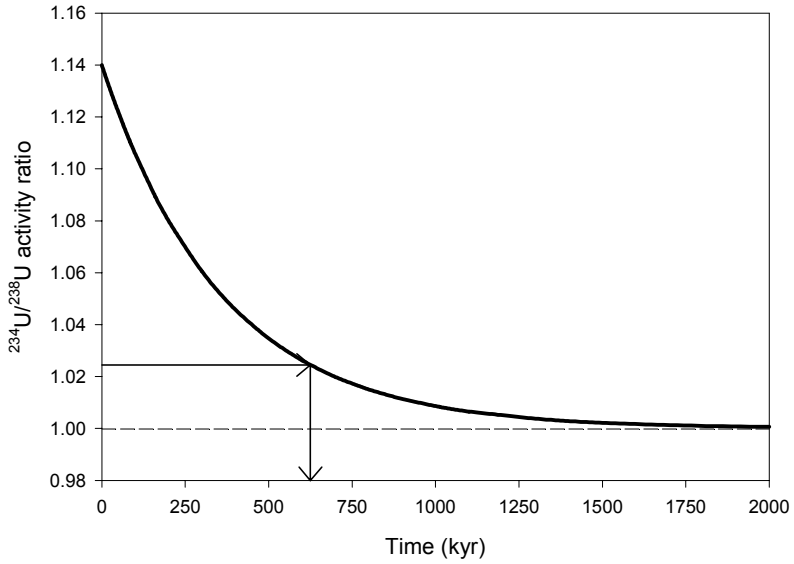

Fig.2.4: *Evolution of the $^{234}U/^{238}U$ activity ratio of marine carbonates (e.g. corals) and the method of age determination by reading the age from the currently measured activity ratio in the marine carbonate.*

While the $^{234}U/^{238}U$ activity ratio in waters is usually >1, the isotopes in unaltered rocks are in secular equilibrium. The ranges for other types of rock and water can be taken from Fig. 2.5.

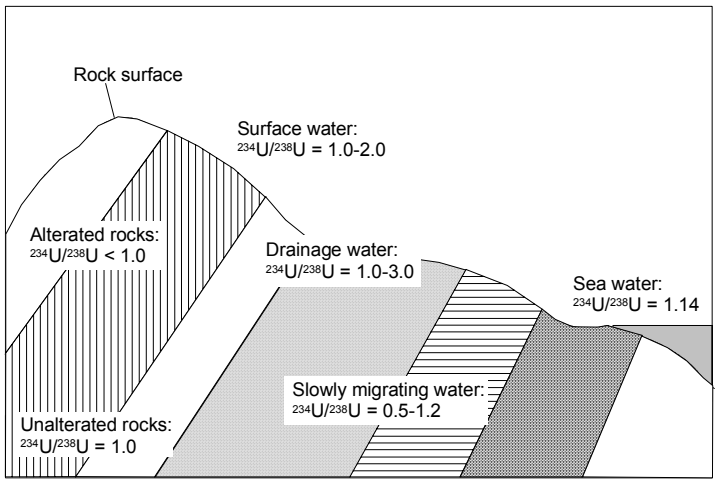

Fig. 2.5: *Generalized view of $^{234}U/^{238}U$ activity ratios in exposed rocks and crustal waters of the continental earth crust (after GASCOYNE, 1992).*

The constant initial value of $^{234}U/^{238}U$ in corals from recent sea water cannot be generalized for secondary calcites from underground solutions. This is why - along with the decay of ^{238}U into ^{234}U - the decay of ^{234}U into ^{230}Th is used as an additional method of age-determination. As thorium is largely immobile and has a short residence time in waters, it is not incorporated into the calcite and the entire thorium measured is ascribed to the disintegration of ^{238}U and ^{234}U into ^{230}Th. Yet, in many calcites ^{232}Th is also detected during isotope measurements. The isotope entered the carbonate sample through contamination e.g. by the surrounding rock ('detrital' Th). Since the detritus may contain uranium as well, a detritus correction of the sample`s isotope data is crucial for its age-determination. Assuming that the carbonate in the sample did not take up any thorium during its formation, only ^{230}Th is measured in the material. Any ^{232}Th will be ascribed to the 'detritus' portion of the sample. It is also important to know the Th/U-concentration ratio for the detritus:

$$\frac{Concentration\,(Th)}{Concentration\,(U)} = 4{,}26 \qquad \text{(Eq. 2.9)}$$

The value 4.26 is the average Th/U-concentration in granites (CHERDYNSTEV 1971) and is often used as a corrective measure for the data. However, to achieve a more precise correction mechanism it is desirable to determine the Th/U-concentration in the surrounding rock. The natural occurrence of thorium is almost exclusively restricted to ^{232}Th; uranium occurs in the form of the isotope ^{238}U with a percentage of 99.27 %. It is therefore possible to rewrite Eq. 2.9 as Eq. 2.14 on the basis of a relation between concentration c, activity A , mass m and the decay constant λ of an isotope i to obtain a correction factor:

$$c_i = \frac{A_i \cdot m_i}{\lambda_i} \qquad \text{(Eq. 2.10)}$$

The numbers 232 and 238 stand for the isotopes ^{232}Th and ^{238}U here.

$$\frac{A\left(^{232}\mathrm{Th}\right)\cdot\frac{m_{232}}{\lambda_{232}}}{A\left(^{238}\mathrm{U}\right)\cdot\frac{m_{238}}{\lambda_{238}}} = 4{,}26 \qquad \text{(Eq. 2.11)}$$

$$\frac{A\left(^{232}\mathrm{Th}\right)}{A\left(^{238}\mathrm{U}\right)} = 4{,}26\cdot\frac{m_{238}}{m_{232}}\cdot\frac{\lambda_{232}}{\lambda_{238}} \qquad \text{(Eq. 2.12)}$$

$$\frac{A\left(^{232}\mathrm{Th}\right)}{A\left(^{238}\mathrm{U}\right)} = 4{,}26\cdot 1{,}0258\cdot 0{,}3189 \qquad \text{(Eq. 2.13)}$$

$$\frac{A(\mathrm{U})}{A(\mathrm{Th})} = 0{,}7175 \qquad \text{(Eq. 2.14)}$$

The product of the two values (^{232}Th-activity of the sample and U/Th-activity ratio) is subtracted from the value measured for the isotope under consideration according to BOLLHÖFER (1996). The activity of the pure calcite sample remains as the adjusted value. Eq. 2.15 illustrates as an example the correction for ^{238}U.

$$^{238}U_{corr.} = {}^{238}U_{meas.} - 0{,}7175 \cdot {}^{232}Th_{meas.} \qquad \text{(Eq. 2.15)}$$

Adjusted values like these can be charted in diagrams suitable for the interpretation of the samples in question. Examples of this sort can be found in later chapters. Most diagrammatic representations of measurement results make it possible to date the samples both graphically and arithmetically.

3 Analyzed samples

3.1 Fracture minerals from the HRL Äspö

The rocks from the Äspö region belong to the Småland-Värmland intrusion; along with the Dalarna and Rätan rocks they form the Southern part of the Trans-Scandinavian granite-porphyry belt (GAAL and GORBATSCHEV 1987). This NNW-orientated belt separates the Svecokarelian belt in the east from the Southwest Swedish gneiss zone in the west. Fig. 3.1. gives a summary of the ages of the Småland-Värmland rocks in comparison to the granites and porphyrites in the rest of the Trans-Scandinavian belt, the Swedish part of the Svecokarelian region, and the gneiss zone in Southwest Sweden.

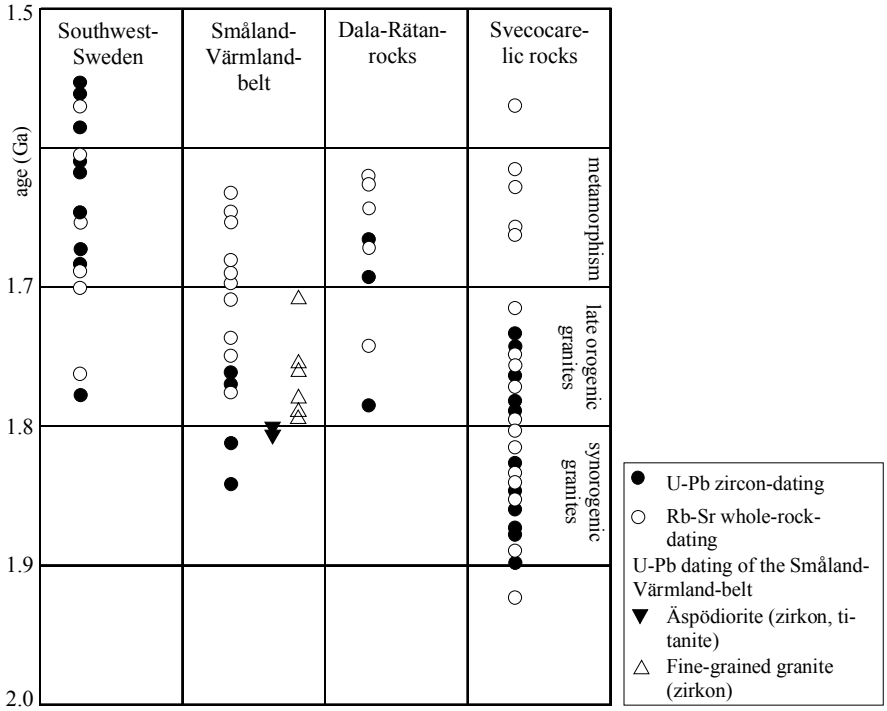

Fig. 3.1: *Published age determinations of rock units of the Småland-Värmland region compared to those of the Dala-Rätan region, SW Sweden and to Svecocarelian units. Data according to JOHANSSON (1988) and KORNFÄLT et al. (1997).*

With the exception of the anorogenic granites all lithologic units have an ENE-WSW-trend and are interpreted as large-scale structures of magmatic flow according to KORNFÄLT et al. (1997). There are also innumerable joints frequently filled with calcite, adular, fluorite, epidote or sheet silicates, which indicate episodic circulation of hydrothermal solutions (LANDSTRÖM and TULLBORG 1995). Similarly, LOUVAT et al. (1999) show that the flow of recent ground water is controlled by the joints and fractures which have a main S-N-trend in the upper 500 m of the HRL Äspö and are cut by many smaller fault and joint systems of varying orientation. STANFORS et al. (1999) found in their isotopic analyses of calcite-dominated fracture fillings that the calcites were not precipitated from today's underground solutions, but have their origin in a number of older hydrothermal events.

3.2 Fracture minerals from the FL Grimsel

Bulk rock age determination of the Central Aar granite by means of the Rb-Sr-method yielded an age of 286 Ma (ALBRECHT and SCHALTEGGER 1988), which is taken to be the intrusion age and thus confirms the Late Variscan age of the Aar granite. KEUSEN et al. (1989) point out that for the Grimsel-granodiorite the whole-rock age could not be established with the Rb-Sr-method. The assumption that the intrusion age of this rock type is 270 to 300 million years is solely based on a U/Pb-dating of zircons.

During the cooling of the rocks and the ensuing loss of volume of the Aar massif, joints were formed within the granite body, which were filled with lamprophyres and occasional aplite dikes. Dating with the Rb-Sr-method established an age of 250 Ma for the aplite dikes (SCHALTEGGER 1987).

The Felslabor in Grimsel consists of a system of tunnels 3.50 m in diameter, totaling 900 m in length (KEUSEN and WEIDMANN 1986). The sites of the 20 fracture filling samples taken from the tunnel walls are shown in Fig. 3.2.

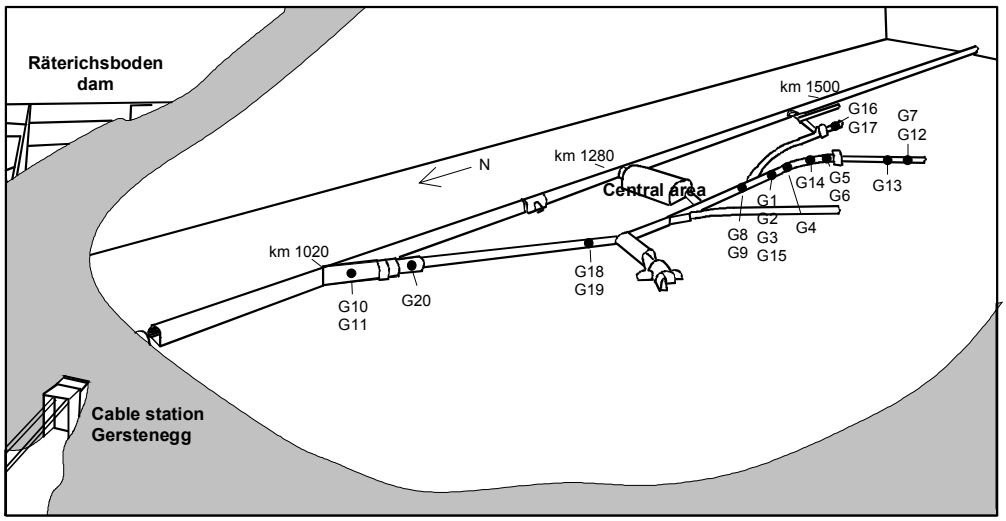

Fig. 3.2: *Sampling sites in the FL Grimsel in a subvertical section (after KEUSEN et al. (1989).*

4 Presentation of analytical results

4.1 ICP-MS analyses

The complete results of the samples analyzed by ICP-MS are listed in GERDES (2000, Appendix Tab. A4, A5). Since the concentrations of U and Th are of particular significance for age determination and secular equilibrium, they are presented in this section (Tab. 4.1):

Tab. 4.1: U and Th concentrations of fracture minerals (HRL Äspö and FL Grimsel)

HRL Äspö calcites			FL Grimsel silicates		
Sample	**Th (ppm)**	**U (ppm)**	**Sample**	**Th (ppm)**	**U (ppm)**
A1	1.66	5.65	G1	0.60	5.27
A2a	2.11	1.69	G2	0.10	1.62
A2b	5.14	3.06	G3	0.08	0.31
A3	0.84	0.48	G4	6.10	2.02
A4	1.96	2.06	G5	0.07	12.85
A5	9.24	2.89	G6	0.07	8.80
A6	3.86	1.26	G8	0.22	0.63
A7	0.79	0.39	G9	0.58	1.45
A8	1.00	1.91	G10	28.53	10.65
A9	13.09	4.03	G11	13.22	4.84
A10	4.66	3.51	G12	0.19	0.20
A11	1.36	1.22	G13	1.31	0.68
A12	0.22	0.41	G14	8.90	3.18
A13	0.35	0.23	G15	3.42	71.29
A19	4.27	2.46	G16	0.21	0.98
A20	3.86	2.20	G17	0.21	0.28
A21	4.62	3.89	G18	2.42	0.64
A22	0.12	0.64	G19	6.99	1.96
A23	5.09	3.93	G20	0.22	0.41
A24	2.48	2.43			
A25	0.46	5.34			
A26	1.01	0.91			
A27a	0.52	0.48			
A28	1.02	0.58			
A29	4.43	1.81			
A30	2.68	1.31			

The data in Tab. 4.1 show that for the samples from the HRL Äspö U-contents range from 0.4 to 5.3 ppm, and Th-contents from 0.1 to 13.1 ppm. Much higher concentrations of U and Th are found in the fracture fillings from the FL Grimsel, with a range from 0.2 to 71.3 ppm for U and from 0.1 to 28.5 ppm for Th. Neither data set reveals a systematic pattern of U- and Th-contents with respect to the minerals contained in individual samples. To assess the validity of the ICP-MS measurements, a granite standard (USGS-G2, GOVINDARAJU 1994) was measured and compared with the set values for the rock in Chapter 11.2 (Tab. 11.1).

4.2 Therm-ion-mass-spectrometry (TIMS) analyses

Samples from the HRL Äspö

The activity ratios of calcites from the HRL Äspö were measured by means of TIMS (Finnegan MAT 262 + RPQ) at the Institute of Environmental Physics of the University of Heidelberg. The data relevant for the analysis are shown in Tab. 4.2.

What is actually represented here is the activity-ratios of the bulk samples, *i.e.* samples with possible silicate components. Silicatic minerals may also contain U and Th, however, so that a correction of the carbonate fraction with respect to the detrital Th seems to be indispensable for the analysis of the data.

Tab. 4.2: Activity ratios of samples from the HRL Äspö. A: calcites, W: underground water. The right column presents the 'detrital' Th/U-ratios ($^{232}Th/^{238}U_{Det}$).

Sample	$^{234}U/^{238}$	$^{230}Th/^{234}$	$(^{232}Th/^{238}U)_D$
A1	0.85	1.10	0.33
A2a	1.32	1.25	6.60
A3	1.49	1.35	6.59
A4	1.73	1.08	6.75
A6	1.55	1.49	3.16
A7	1.48	1.06	3.31
A8	1.44	1.03	1.01
A11	1.06	1.09	3.42
A12	1.47	1.07	-
A13	1.11	1.14	-
A19	1.22	1.06	3.38
A20	1.57	1.06	2.15
A22	2.13	0.88	-
A23	0.79	4.63	2.44
A24	1.01	1.04	1.12
A25	0.89	0.98	0.14
A27a	2.14	0.60	1.89
A30	2.08	1.24	5.52
A31	2.78	0.75	1.78
W1	4.32	0.00	-
W2	4.49	0.00	-
W3	3.90	0.00	-

This correction procedure will be demonstrated using sample A 20; the necessary formulae were already described in Chapter 2 (Eq. 2.9 - 2.15). Such a detritus correction does not only require the specification of the ^{232}Th-activity of the sample, but also that of the Th/U-concentration ratio of the surrounding rock. Assuming that the sample material, due to the preparation of the calcite, has taken up some of the silicate components, we considered a component-sensitive dissolution of the sample necessary. The purpose of this dissolution is to separate the silicate fraction, which is largely insoluble in dilute acid, from the calcite component. This method draws upon the approach in GERDES (2000) which describes the optimum way to separate carbonate and silicate fractions in impure calcites and is briefly reported here: A Teflon™ crucible

is loaded with 100 mg of the sample, 6 ml of hydrochloric acid with a molar concentration of 0.0005 is added and the sample solution is shaken overnight. Since the concentration of the acid is so low, it is safe to assume that no U or Th is dissolved out of the silicate component. Subsequent centrifuging and decanting of the solution separates it from the insoluble fraction, which is then dried. The silicate residue undergoes pressure-induced dissolution (180°C, 6 hours) with 3 ml of HF and $HClO_4$ each, and the U and Th concentrations of the solution are analyzed by means of ICP-MS.

The following calculations for sample A 20 are a representative example. A Th/U-ratio of 2.15 was measured for this calcite, the values for the other samples are listed in Tab. 4.2. The Th/U-concentration ratio of A 20 is converted into a U/Th-activity ratio using the Eq. 2.15.

$$\frac{A\left(^{232}Th\right)}{A\left(^{238}U\right)} = 2.15 \cdot 1.0258 \cdot 0.3189 \qquad \text{(Eq. 4.1)}$$

$$\frac{A(Th)}{A(U)} = 0.7046 \qquad \text{(Eq. 4.2)}$$

$$\frac{A(U)}{A(Th)} = 1.4192 \qquad \text{(Eq. 4.3)}$$

The resulting value 1.4192 is the correction factor with which the isotopes ^{234}U, ^{238}U and ^{230}Th of the sample are corrected. The individual activities of these isotopes and that of ^{232}Th for the sample A 20 are shown in Tab. 4.3.

Tab. 4.3: Uncorrected activity ratios of sample A20 (dpm/g= decay per minute and gram).

	^{234}U	^{238}U	^{230}Th	^{232}Th
Activity [dpm/g]	2.57	1.64	2.71	0.89

On the basis of Eq. 2.15 the corrections of the isotopes are worked out as follows:

$^{234}U_{corrected} = {}^{234}U_{measured} - \text{correction factor} \cdot {}^{232}Th_{measured}$

$^{234}U_{corrected} = 2.57 - 1.4192 \cdot 0.89$

$^{234}U_{corrected} = 1.31$ dpm/g

$^{238}U_{corrected} = 0.38$ dpm/g

$^{230}Th_{corrected} = 1.45$ dpm/g

The corrected values for the activity and activity ratios for sample A 20 are listed in Tab. 4.4.

Tab. 4.4: Corrected activities (in dpm/g) and activity ratio of A20.

^{234}U	^{238}U	^{230}Th	$^{234}U/^{238}U$	$^{230}Th/^{234}U$
1.31	0.38	1.45	3.43	1.11

In some samples the insoluble fraction was too small for a dissolution of the detritus. In these cases the mean value of all analytical results (2.4) was used to determine the Th/U-ratio of each sample. STOSNACH (1999) carried out bulk rock analyses of Småland granite and Äspö diorite and established 2.3 as mean value for the Th/U-ratio, so that obviously the dissolution with 0.005 M hydrochloric acid mentioned above is well suited to the separation of the silicate matrix. Tab. A7 in the Appendix of GERDES (2000) contains the corrections for the calcites, the corrected activity ratios of the whole set of samples are listed in Tab. 4.5.

Tab. 4.5: Activity ratios corrected for detrital Th of calcites from the HRL Äspö.

Sample	$^{234}U/^{238}U$	$^{230}Th/^{234}U$
A1	0.58	1.39
A2a	1.40	1.29
A3	1.52	1.43
A4	2.19	1.10
A6	1.56	1.44
A7	2.40	1.11
A8	3.64	1.08
	1.08	1.11
A12	1.55	1.07
A13	1.16	1.21
A19a	2.37	1.20
A20	3.43	1.11
A22	2.21	0.87
A23	0.61	9.66
A24	1.07	1.25
A25	0.75	0.95
A27a	4.49	0.42
A30	2.73	1.22
A31	5.38	0.68
W1	4.32	0.00
W2	4.49	0.00
W3	3.90	0.00

Calcites and silicates from the FL Grimsel

The activity ratios of calcites and silicates from the FL Grimsel were measured with a TIMS (Finnegan MAT 262 + RPQ) at GEOMAR in Kiel. Tab. 4.6 shows the results that are immediately relevant to our analysis, the rest of the data has been compiled in Tab. A9 in the Appendix of GERDES (2000). The data in Tab. 4.6 again are the TIMS measurement results from which the blank values have already been subtracted.

Tab. 4.6: Activity ratios of samples from the FL Grimsel. Samples denominated -S: silicate dominated fracture material, samples denominated -C: calcite dominated fracture material.

Sample	$^{234}U/^{238}U$	$^{230}Th/^{234}U$
G1-S	1.10	0.31
G2-C	1.08	0.06
G3-C	1.21	0.76
G5-C	1.12	0.01
G8-S	1.69	0.13
G9-S	1.15	0.11
G10-C	1.02	1.25
G11-C	1.04	0.94
G13-C	1.25	0.13
G14-S	1.04	0.54
G15-C	1.22	0.15
G16-C	1.92	0.55
G18-S	1.06	0.94
G19-S	1.03	1.05

Unlike the calcites from the HRL Äspö, the FL Grimsel samples do not require correction for the detrital ^{232}Th. The mixing ratio of newly formed minerals and the silicate component in the samples is important, though, and it is this ratio that could be affected by detritus correction.

5 Model calculations of U/Th isotopic evolution

5.1 Samples from the HRL Äspö

The results of recent research on the formation of fracture fillings in the HRL Äspö by WALLIN and PETERMAN (1999) and STANFORS et al. (1999) are the following: The analysis of carbon-, oxygen- and strontium isotopes of calcites received from deep drill cores has shown that for samples taken from sites about 900 m deep or more the carbon and the oxygen isotopes of the carbonate suggest a rather old age of formation (>1 Ma). In shallower granite sections, the $\delta^{13}C$-values for the calcites indicate clearly that surface waters contributed to their formation. WALLIN and PETERMAN (1999) interpret these observations in such a way that calcites were formed from shallower solutions during the past glacial periods. STANFORS et al. (1999) take the fracture mineralization in the HRL Äspö as a sign that, along with new formations, there are also minerals which are the result of the dissolution/precipitation of pre-existing calcites. These observations suggest two general hypotheses for the problems under consideration here:

1. **Preglacial calcites**, i.e. those older than one million years, have been altered with respect to their U- and Th-isotopy due to their contact with migrating underground solutions. Since it is not possible to tell exactly if these calcites are one million years old or possibly much older, it is assumed that the $^{234}U/^{238}U$- and $^{230}Th/^{234}U$-ratios were in secular equilibrium at the time of calcite redissolution or recrystallization. These redissolution and recrystallization processes (isotopic disturbances) will be discussed below as Cases A,B and C and will be considered in more detail in Chapter 6.1.1.
2. For **recent calcites** WALLIN and PETERMAN'S (1999) position is adopted, according to which calcites were formed from near-surface underground solutions in the past 800 ky, i.e. during glacial periods. These newly formed calcites do not require redissolution or recrystallization. They incorporated the uranium isotope ratio of the underground solution in their crystal lattice and have developed towards a secular equilibrium ever since. This recent formation of calcites will be discussed as Case D.
3. Finally it is quite conceivable that recently formed calcites have undergone a disturbance in their U/Th-isotopy during their development towards the secular equilibrium. This last possibility will be considered as Case E. Cases D and E will be more closely examined in Chapter 6.1.2.

5.1.1 Model of preglacial calcite formation

With the exception of the samples of Case D, which describes the primary, undisturbed formation of calcites, a model for the simulation of a disturbance of the isotope ratios will be set up for the samples from the HRL Äspö. The following discusses the development of this model and the equations used in it. On account of earlier measurements of the uranium contents of the HRL Äspö samples and geological estimates it is assumed that 5 ppm uranium with an initial $^{234}U/^{238}U$-activity ratio 5 was incorporated during the calcite formation process.

The derivations of the equations used in this model can be found in appendix A of GERDES (2000). The number of ^{238}U atoms at a time t is determined by the initial quantity ($^{238}U_{event}$) on the one hand and the decay ($e^{-\lambda t}$) on the other (Eq. 5.1).

$$^{238}U = {}^{238}U_{event} \cdot e^{-\lambda_{238} t} \qquad \text{(Eq. 5.1)}$$

$^{238}U_{event}$ denotes the quantity of this isotope immediately after the disturbance ('event') and the termination of the secular equilibrium tied up with it. The ^{238}U decay is not affected by the disturbance since selective migration of ^{234}U has no influence on the concentration of the mother isotope.

The number of ^{234}U atoms can be determined with the help of Eq. 5.2, described in BATEMAN (1910).

$$^{234}U = {}^{238}U_{event} \cdot \frac{\lambda_{238}}{\lambda_{234} - \lambda_{238}} \cdot \left(e^{-\lambda_{238} t} - e^{-\lambda_{234} t} \right) + {}^{234}U_{event} \cdot e^{-\lambda_{234} t} \qquad \text{(Eq. 5.2)}$$

The first term in Eq. 5.2 signifies the number of ^{234}U atoms that result from the decay process within the time span t since the disturbance event. The actual disturbance of the system is simulated by $^{234}U_{event}$. Therefore, the last term of the equation describes the number of the ^{234}U atoms affected by the disturbance which have undergone decay into ^{230}Th in the time period t since the disturbance event.

Following BATEMAN (1910) the number of ^{230}Th atoms generated in the course of time can be calculated with Eq. 5.3.

$$^{230}Th = {}^{238}U_{event} \lambda_{238} \lambda_{234} \left(\frac{e^{-\lambda_{238} t}}{(\lambda_{234} - \lambda_{238})(\lambda_{230} - \lambda_{238})} + \frac{e^{-\lambda_{234} t}}{(\lambda_{238} - \lambda_{234})(\lambda_{230} - \lambda_{234})} \right.$$

$$\left. + \frac{e^{-\lambda_{230} t}}{(\lambda_{238} - \lambda_{230})(\lambda_{234} - \lambda_{230})} \right) + {}^{234}U_{event} \cdot \frac{\lambda_{234}}{\lambda_{230} - \lambda_{234}} \cdot \left(e^{-\lambda_{234} t} - e^{-\lambda_{230} t} \right)$$

$$+ {}^{230}Th_{event} \cdot e^{-\lambda_{230} t} \qquad \text{(Eq.5.3)}$$

The first term of Eq. 5.3 designates the number of atoms ^{230}Th which are the result of the decay of ^{238}U in the time t since the disturbance. The second term shows the number of ^{230}Th atoms that have been generated through the decay of ^{234}U affected by the disturbance. The third term can be neglected for the new formation of calcite since in this case no ^{230}Th is incorporated initially.

Eqs. 5.1 to 5.3 make it possible to describe a disturbance of the ^{234}U concentration and the subsequent decay of the isotopes ^{238}U, ^{234}U and ^{230}Th. Fig. 5.1 shows the two cases of selective gain (Case A, closed symbols) and selective loss (Case B, open symbols) of ^{234}U starting from the state of secular equilibrium in a $^{234}U/^{238}U$ – $^{230}Th/^{234}U$ activity diagram.

The equations will be discussed in Chapter 6.1.1. The effect of the disturbance of the migrating solutions is a deviation of the samples in the diagram from the state of secular equilibrium. Subsequent decay causes the calcites to gradually decay into their initial state of equilibrium. The change of concentration for Case A is assumed to be a gain of ^{234}U by a factor of 2 (degree of disturbance = 2), and for Case B a loss of 30 % ^{234}U (degree of disturbance = 0.7).

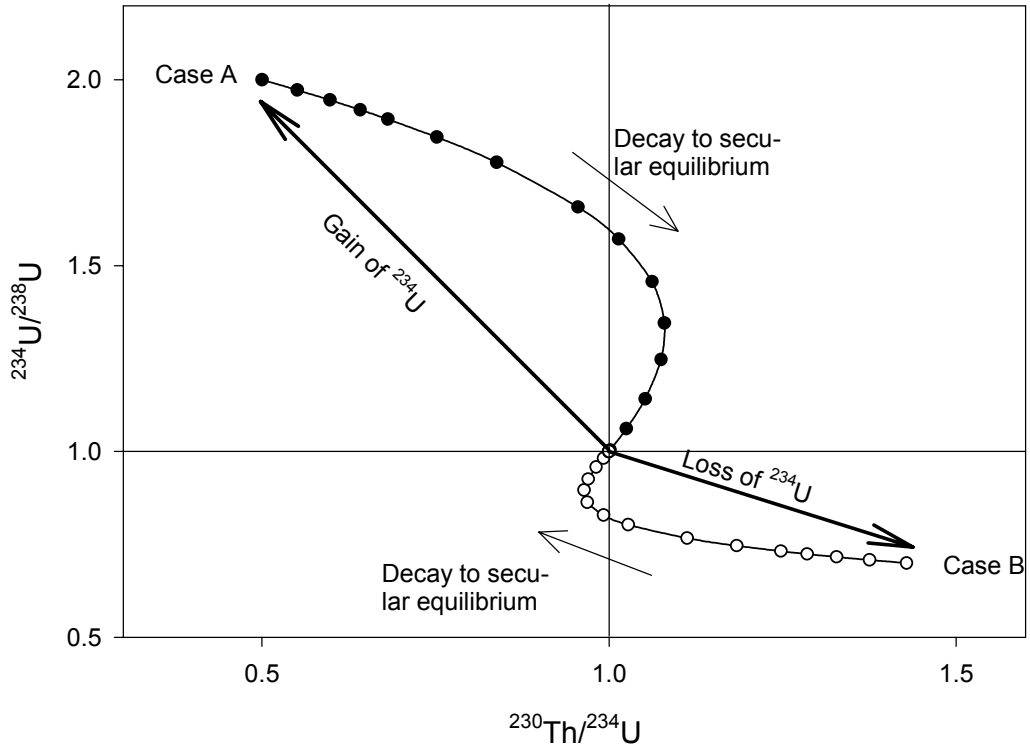

Fig. 5.1: *Principles of ^{234}U loss and gain and disturbance of the secular equilibrium of calcite in a $^{234}U/^{238}U$-$^{230}Th/^{234}U$ activity diagram. Case A: two-fold enrichment of ^{234}U (degree of disturbance=2), Case B: 30 % loss of ^{234}U (degree of disturbance=0.7).*

Fig. 5.2 shows the result of extending the range of values in Fig. 5.1, which is a gain of ^{234}U by factors from 1.5 to 7 for Case A (closed symbols), and a loss of 10 to 90 % of ^{234}U for Case B (open symbols).

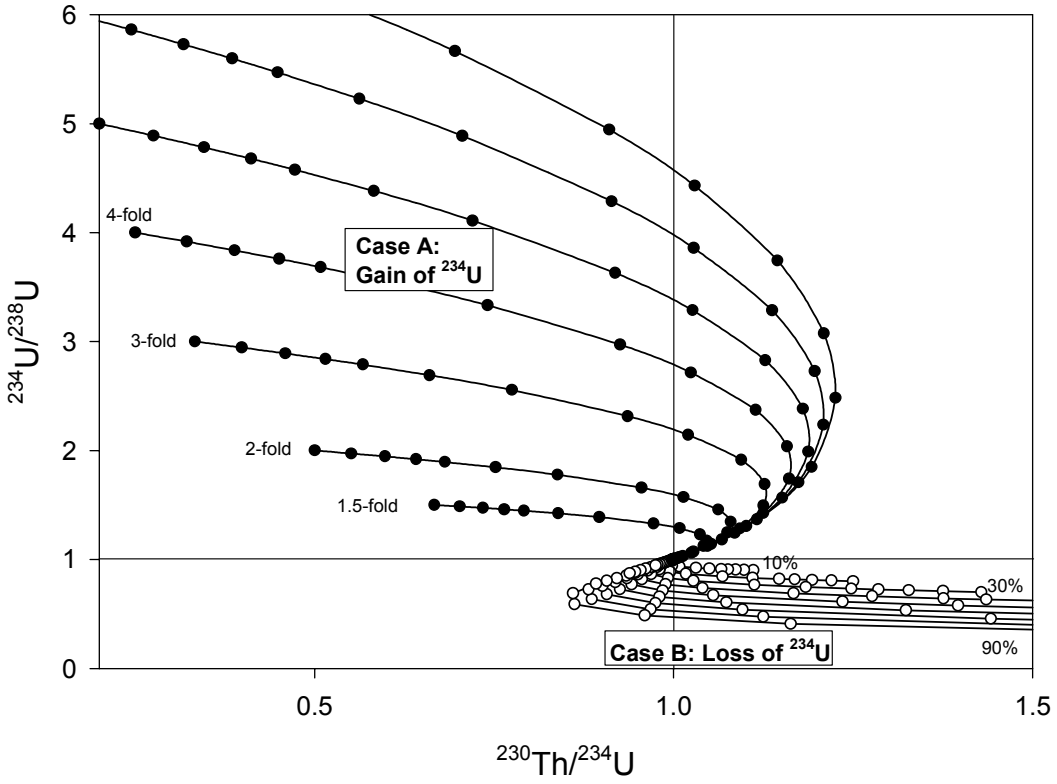

Fig. 5.2: *Principles of ^{234}U loss (open symbols) and gain (closed symbols) and at different degrees of disturbance of the secular equilibrium. Case A: two-fold enrichment of ^{234}U: Case A: 1.5-fold to 7-fold enrichment in ^{234}U , Case B: 10 to 90 % loss of ^{234}U corresponding to degrees of disturbance of 0.9 to 0.1.*

Isochrons can be incorporated in Fig. 5.2. Therefore, it is possible to assess both the temporal sequence and the degree of disturbance of a given sample (see Fig. 5.3). Strictly speaking, the value of the temporal assessment does not specify the age of the samples formation, but rather the time that has passed since the last disturbance of the evolving or already evolved equilibrium.

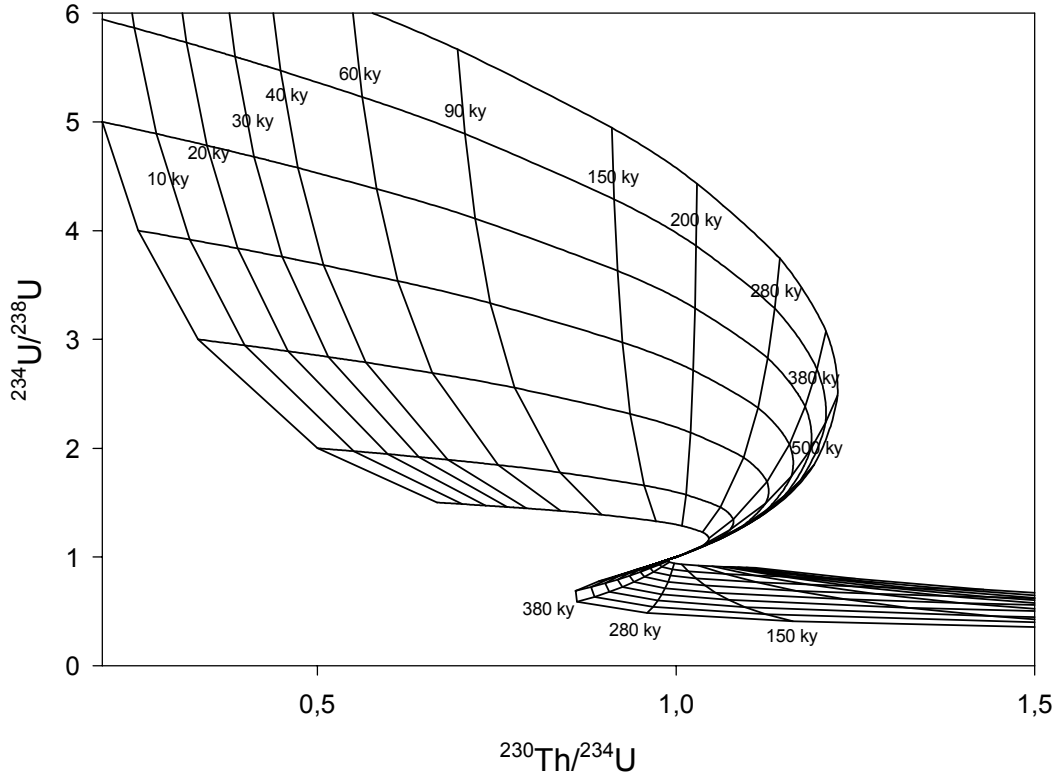

Fig. 5.3: *Isochron diagram for ^{234}U loss and gain in a $^{234}U/^{238}U$-$^{230}Th/^{234}U$ activity diagram. The near-vertical lines correspond to secular evolution of a disturbed sample in ky.*

5.1.2 Model of recent calcite formation

A diagram worked out by KAUFMAN and BROECKER (1965), which sets off the activity ratios of $^{234}U/^{238}U$ against those of $^{230}Th/^{234}U$, is suitable for the representation of samples subject to the conditions of recent formations. It is based on the following equations calculating decay:

$$\frac{A\left(^{230}Th\right)}{A\left(^{234}U\right)} = \frac{1-e^{-\lambda t}}{\frac{A\left(^{234}U\right)}{A\left(^{238}U\right)}} + \left(1-\frac{1}{\frac{A\left(^{234}U\right)}{A\left(^{238}U\right)}}\right)\cdot\frac{\lambda_{230}}{\lambda_{230}-\lambda_{234}}\cdot\left(1-e^{-\left(\lambda_{230}-\lambda_{234}\right)t}\right)$$

(Eq. 5.4)

$$\frac{A\left(^{234}U\right)}{A\left(^{238}U\right)} = \left[\left(\frac{A\left(^{234}U\right)}{A\left(^{238}U\right)}\right)_{initial} - \frac{\lambda_{234}}{\lambda_{234}-\lambda_{238}}\right] \cdot e^{-\left(\lambda_{234}-\lambda_{238}\right)t} + \frac{\lambda_{234}}{\lambda_{234}-\lambda_{238}}$$

(Eq. 5.5)

Taking into account the necessary boundary conditions for a closed system of U/Th mobilization and assuming that the samples have not incorporated any ^{230}Th, the following diagram is derived from Eqs. 5.4 and 5.5 as a result:

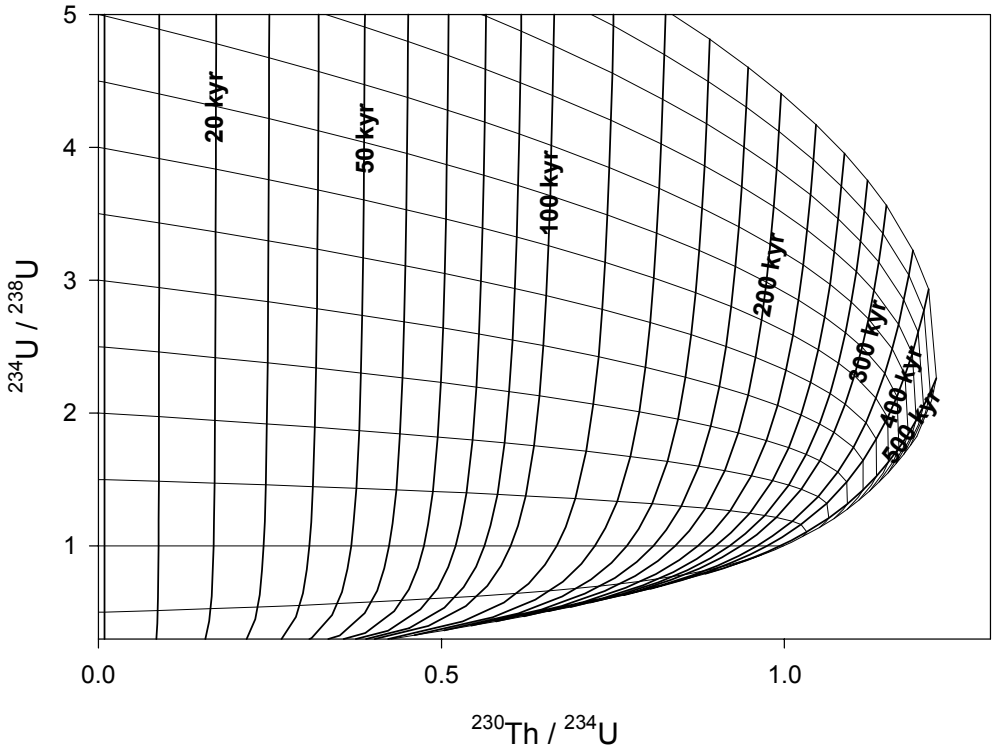

Fig. 5.4: *Isochron diagram for $^{234}U/^{238}U$ and $^{230}Th/^{234}U$ activity ratios according to KAUFMAN und BROECKER (1965). The near-horizontal lines are growth curves, the near-vertical lines represent isochrons.*

The near vertical lines in Fig. 5.4 represent isochrons relative to variable $^{234}U/^{238}U$-activity ratios. The near horizontal lines are growth curves which indicate the change of isotope ratios for the initial $^{234}U/^{238}$-ratios in the course of time. If carbonate is formed from an aqueous solution and uranium incorporated in the form of uranyl-carbonate complexes, the evolution of the sample starts at a given $^{234}U/^{238}U$- ratio at the ordinate of the diagram (no ^{230}Th present). Over time, the sample develops towards secular equilibrium along the near horizontal decay curve. The time since the formation of the sample and its initial $^{234}U/^{238}U$- activity ratio can either be determined graphically through Fig. 5.4 or calculated with the help of Eqs. 5.4 and 5.5.

5.2 Samples from the FL Grimsel

According to KEUSEN et al. (1989), the geological situation in the FL Grimsel suggests that the fracture fillings found there (e.g. chlorite, quartz) are of late alpidic origin (Miocene/Pliocene). This means that the analyzed samples containing such minerals cannot be interpreted as recent formations, but must be taken to be old fracture fillings which once were in secular equilibrium and whose isotope ratios have been disturbed by external processes. Two cases can be distinguished here:

1. In the first case a system of rock assemblages is assumed which is open to changes in the U/Th isotope ratios. Unlike the samples from the HRL Äspö, the disturbances of the secular equilibrium of the Grimsel samples are not solid-solution-reactions, but rather activities due to the influence of adjacent rock on the isotope ratios of the fracture filling (**solid-solid-reaction**). In the adjacent rock as well as the fracture mineral itself continuous processes are at work that allow ^{234}U and ^{230}Th isotopes to migrate out of their primary site, after their lattice has been disturbed through the α-recoil of the mother isotope. On the assumption that the geometrical body in which decay takes place is a sphere and that an atom can survive up to ten collisions, the average possible percentage of atoms leaving this body can be determined. This value is ca. 28 % according to SCHEID (1979). If the uranium concentration in both volumes (fracture mineral and surrounding rock) is approximately the same, the ^{234}U and ^{230}Th isotopes will move with an equal share of 28 % from the neighboring rock into the fracture filling and vice versa. Both the amount and the direction of selective ^{234}U and ^{230}Th gain is thus controlled by the difference of uranium concentrations in both the rock and the vein mineral. These alteration processes will be dealt with as Case F and G below; the samples that go with them will be considered in more detail in Chapter 6.2.1.

2. In the second case a system is confined to the vein which is closed with respect to isotope ratios and in which a **solid-solution-reaction** takes place. Unlike the samples from the HRL Äspö, the fracture fillings sampled in the FL Grimsel are not exclusively calcites, but include silicates (e.g. chlorites and quartz) as well. Assuming a closed system within the vein and a state of secular equilibrium for all samples, the calcites and silicates can influence each other with respect to their U/Th-isotope ratios when they are infiltrated by a solution. The reason for this is the difference in the dissolution behaviour of minerals. This can be illustrated with the help of Fig. 5.5.

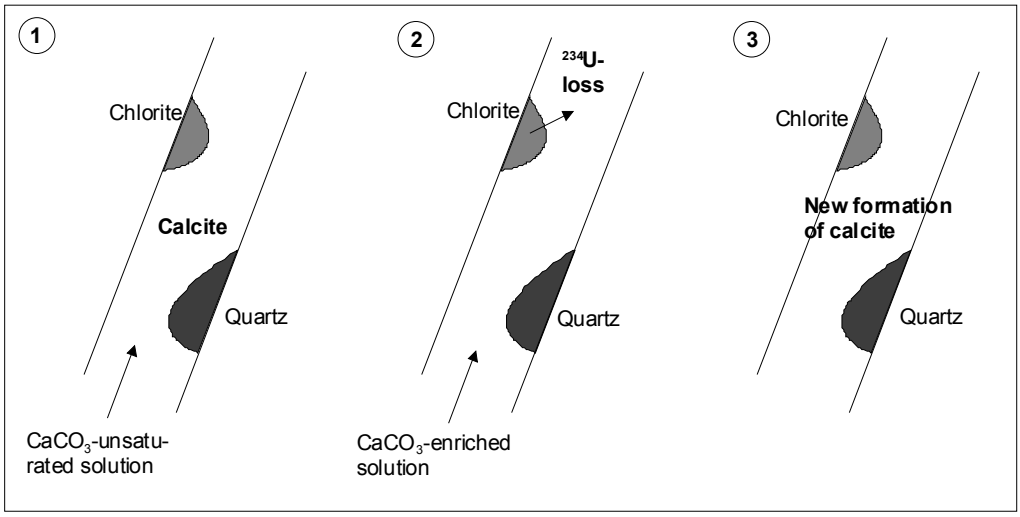

Fig 5.5: *Schematic sketch of water/rock interactions in a model fracture. 1: The fracture filling consists of chlorite, quartz, and a calcite matrix.* $^{234}U/^{238}U$ *and* $^{230}Th/^{234}U$ *activity ratios are in secular equilibrium, a* $CaCO_3$*-undersaturated solution enters the fracture and dissolves the calcite. Due to their low solubility in this solution, chlorite and quartz remain in place. 2:* ^{234}U *from the chlorite enters the solution and the mineral chlorite hence is depleted in* ^{234}U*. 3: A* $CaCO_3$*-saturated solution entering the fracture precipitates new calcite in the fracture.*

As indicated in Fig. 5.5, the starting point is a calcite vein which also contains silicate minerals, e.g. chlorite and quartz. Chlorite is taken to be a typical instance of a mineral with a relatively high uranium content here; the concentration of uranium in quartz can be considered very low. If a $CaCO_3$-undersaturated solution enters the vein, it dissolves the calcite partially or completely (position 1 in Fig. 5.5). Due to the insolubility of the silicate minerals in aqueous solutions, chlorite and quartz remain unaltered during this process. The α-recoil of the mother isotope has weakened the lattice structure bonds of ^{234}U in the silicate mineral chlorite, which is therefore the isotope that migrating solutions prefer to take up and remove. The result is a selective loss of ^{234}U in the calcite. In quartz, this process does not occur or occurs only to a very limited degree as a consequence of the low SiO_2 solubility and the low U-concentration (position 2 in Fig. 5.5). A $CaCO_3$-saturated solution entering an open vein created this way can trigger the formation of new calcite (position 3 in Fig. 5.5). If the whole sample taken from the vein is dissolved, both the calcite and silicate minerals find their way into the solution to be analyzed. Therefore, a combination of three processes is observed: calcite which has incorporated U with a concentration of a few ppm, but no Th whatsoever; chlorite which has undergone ^{234}U-loss after it was in a state of secular equilibrium; and finally quartz whose isotope ratios remained in secular equilibrium during the disturbance. The consequences of these processes for FL Grimsel samples are discussed in Chapter 6.2.2.

5.2.1 Model of solid-solid-reactions

The centerpiece of the model based on the late alpidic origin of fracture fillings is the weakening of the lattice structure bonds of the isotopes ^{234}U and ^{230}Th due to α-recoil effects and their migration into neighbouring rock. Apart from the case that the uranium concentrations of both the fracture filling and the neighbouring rock are approximately the same and therefore neither the gain nor the loss of an isotope is recognizable, two more cases can be distinguished:

Case A: If the uranium concentration of the neighbouring rock is higher than that of the vein mineral, more ^{234}U is produced in the neighbouring rock than in the vein. This ^{234}U migrates into the vein mineral as a result of the α-recoil effect and disturbs the isotope ratios of the samples there. Furthermore, the ^{234}U now incorporated in the vein mineral in turn decays to ^{230}Th, which thereby moves back again into the neighbouring rock. Thus not only does the amount of ^{234}U in the vein mineral increase, but the amount of ^{230}Th decreases at the same time. This selective gain of ^{234}U and loss of ^{230}Th is mirrored in the isotope ratios of the vein mineral, where the $^{234}U/^{238}U$-ratio becomes greater and the $^{230}Th/^{234}U$-ratio smaller. Fig. 5.6 sketches the evolution of this disturbance in a $^{234}U/^{238}U$-$^{234}U/^{230}Th$ activity-ratio diagram. It should be noted here that the relative portions of ^{234}U-gain and ^{230}Th-loss are variable during the disturbance (represented through the double arrows in Fig. 5.6). It is thus possible to identify different sets of samples with a different relation between ^{234}U-gain and ^{230}Th-loss each in the diagram, and with it different isotope evolutions.

Case B: If the uranium concentration of the vein mineral is higher than that of the neighbouring rock, the same process applies in the opposite direction. The result is that the$^{234}U/^{238}U$-activity ratio becomes smaller and the $^{234}U/^{230}Th$ activity-ratio greater. This effect is also shown in Fig. 5.6.

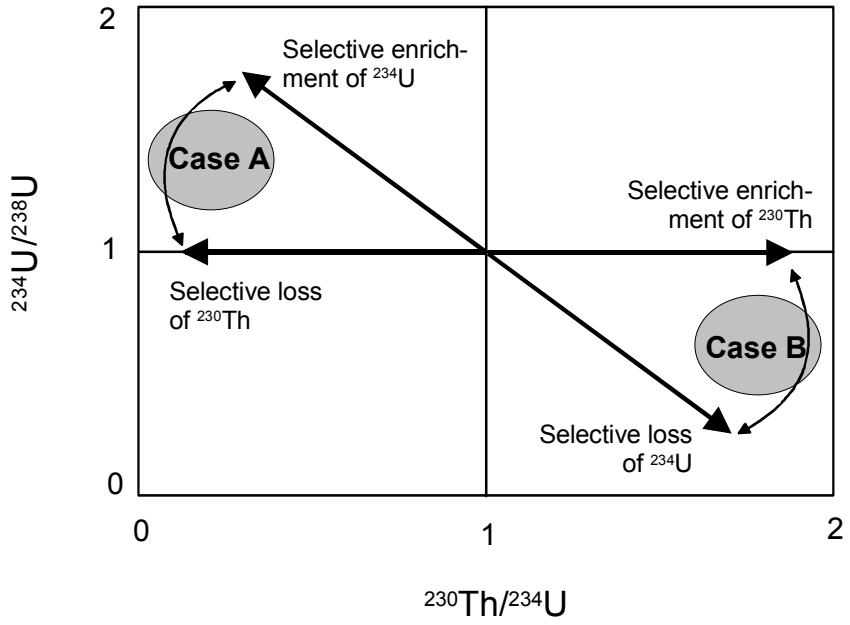

Fig. 5.6: *Principle effects of gain and loss of ^{234}U und ^{230Th} in a solid/solid reaction caused by α-recoil of ^{234}U und ^{230}Th in fracture minerals and the surrounding rock matrix.*

The disturbances of the secular equilibrium of vein minerals mentioned above are therefore not taken to be a type of unique, quick disturbance of the isotope ratios, but rather a system open to isotope migrations within rock assemblages. This is the reason why a determination of the age of the Grimsel samples, which are based on the model of an open vein system, is not possible. Therefore, in Chapter 6.2.1 only the principal isotope evolutions of such FL Grimsel samples will be assessed.

5.2.2 Models of solution-solid-reactions

Recently formed calcites (Case C): A suitable basis for the recently formed calcites in the vein in the FL Grimsel is the diagram according to KAUFMANN and BROECKER (1965), which was already described in 6.1.2. With the help of the Eqs. 5.4 and 5.5 a $^{234}U/^{238}U$-$^{230}Th/^{234}U$ activity diagram is set up which makes it possible to determine both the formation age and the initial $^{234}U/^{238}U$- activity ratio of the fracture mineral.

Chlorites with selective loss of ^{234}U (Case D): The model of selective loss of ^{234}U described in 6.1.1 lends itself to the representation of uranium-rich fracture minerals. The simulation of removal of ^{234}U by means of Eqs. 5.1 to 5.3 enables the determination of the age as well as the degree of the disturbance for a given sample.

Quartz in secular equilibrium (Case E): The isotope ratios of fracture minerals with a low content of uranium are not altered in a disturbance through migrating solutions. Thus, they remain in secular equilibrium with their activity ratios $^{234}U/^{238}U = 1$ and $^{230}Th/^{234}U = 1$ and will therefore be neglected for the further analysis of the evolution of isotopes during the disturbance.

The values of the $^{230}Th/^{234}U$-activity ratios for the Grimsel samples which have been analyzed by TIMS vary considerably. This means that with respect to the representation of recently formed calcites in a $^{234}U/^{238}U$-$^{230}Th/^{234}U$ activity diagram the formation ages of the samples spread over a range of 1 ky and 300 ky. Since such grossly varying ages seem to be highly improbable for a space as narrow as the tunnel at Grimsel, it is safe to assume that most of the samples are a mixture of two of the cases mentioned above. Fig. 5.7 outlines the three cases and, in an exemplary fashion, the resulting U/Th isotope evolutions in a $^{234}U/^{238}U$-$^{230}Th/^{234}U$ activity diagram.

It follows that the position of a sample in Fig. 5.7 does not depend on its isotope evolution (and hence its age), $^{234}U/^{238}U$- activity ratio and character of the disturbance alone, but also on the mixing ratio of recently formed calcite and older silicate minerals. The mixing ratio of the samples is unknown; hence it is impossible to derive any exact age determination of the fracture minerals. Therefore, the ages recorded are rather maximum formation ages which have been blurred by the influence of silicate minerals, which are nearly insoluble in migrating underground solutions.

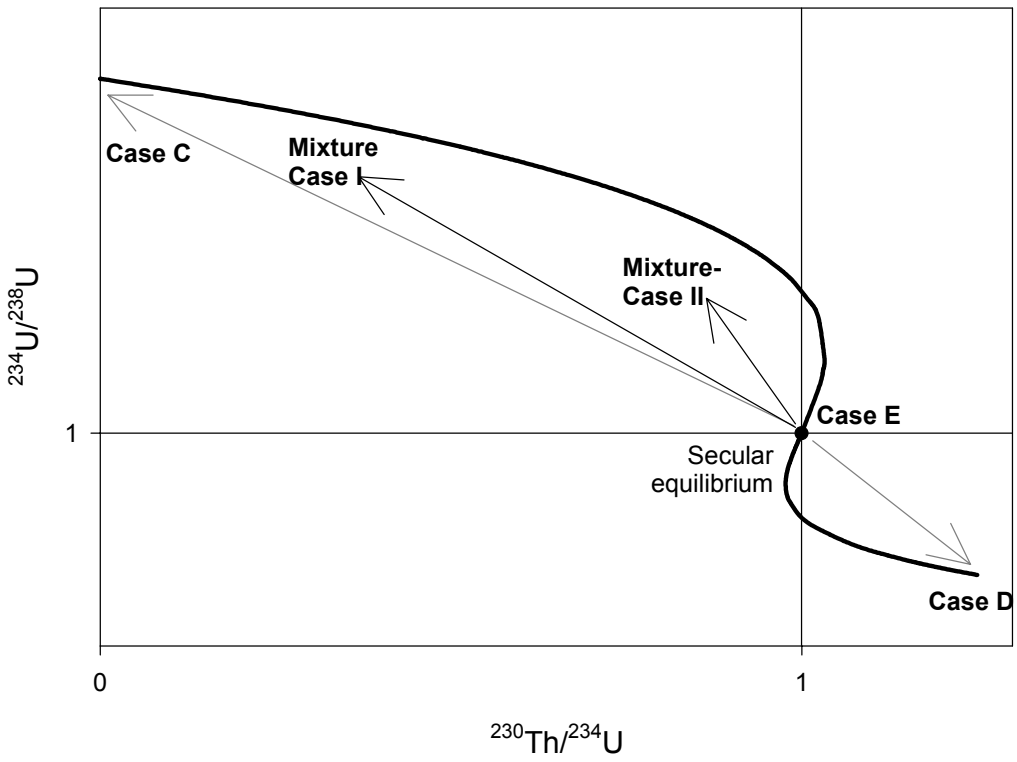

Fig. 5.7: *Principles of the evolution of activity ratios in a mixture of minerals which have been subjected to reaction with a migrating underground solution resulting in specific ^{238}U depletion and precipitation of new calcite. Case C: Formation of calcite. Case D: Loss of ^{234}U from a silicate mineral to the solution. Case E: Undisturbed secular equilibrium of a U-poor mineral which experienced different mixtures with new calcite: Mixture I: Small amounts of silicate (depleted in ^{234}U) with large amounts of new calcite. Mixture II: Large amounts of silicate (depleted in ^{234}U) with small amounts of new calcite.*

6 Dating of fracture mineral formation and U/Th isotope disturbances

6.1 Samples from the HRL Äspö

The Cases A to E outlined in Chapter 5 lead to a very complex picture when it comes to the interpretation of analytical data of fracture calcites and the mobility of uranium and thorium in fracture mineralization of the HRL Äspö. In the following a discussion of the different cases and descriptions of the effects of the reaction with underground solutions will be presented in more detail.

6.1.1 Model of preglacially formed calcites

Three cases (A,B,C) of underground solutions having an impact on the sampled calcites can be distinguished:

Case A: If a saline CO_3-rich but undersaturated underground solution meets a calcite fracture filling, a local $CaCO_3$-saturation is achieved at the solution-calcite interface through dissolution-precipitation processes. The calcite veins investigated here consist of individual microcrystalline calcites, all of them with phyllo-silicate impurities. Crystal agglomerates like these have a large internal surface and therefore a great potential for the local $CaCO_3$-dissolution-precipitation reaction. In this process the calcite gains uranium from the underground solution, and its $^{234}U/^{238}U$-activity ratio is that of the migrating solution. The $^{234}U/^{238}U$-ratio in recent underground solutions from Äspö is also considerably higher than 1, as shown in Tab. 4.3. The process described here disturbs the uranium isotope ratio of a calcite in secular equilibrium, which after completion of the dissolution/precipitation reaction depicted above again starts to achieve secular equilibrium.

Case B: If a solution undersaturated with $CaCO_3$ meets a calcite vein at another point in the Äspö granite rock, it specifically gains ^{234}U. This process, too, is a long-standing observation (e.g. KIGOSHI 1971), which explains the $^{234}U/^{238}U$-activity of 1.14 of recent sea water, for example. In this case a solid with a deficiency of the daughter isotope ^{234}U remains. After the completion of the reaction a secular equilibrium has to be reestablished through an increase in the ^{234}U-activity.

Case C: In addition to the two processes described as A and B a combination of these is possible in which calcites in the state of secular equilibrium first gain ^{234}U and then redevelop towards this state in a closed system over a longer period of time. Before equilibrium has been reached, however, another disturbance of the system occurs with the result that ^{234}U is transferred to a migrating underground solution due to α-recoil effects.

Fig. 8.1 sketches the three cases in a $^{234}U/^{238}U$-$^{230}Th/^{234}U$ activity diagram. Field A represents the result of ^{234}U-gain, field B that of ^{234}U-loss, taking secular equilibrium to be the initial state in either case. Field C represents both these cases occurring in combination. The activity of ^{230}Th remains constant in all cases of disturbances.

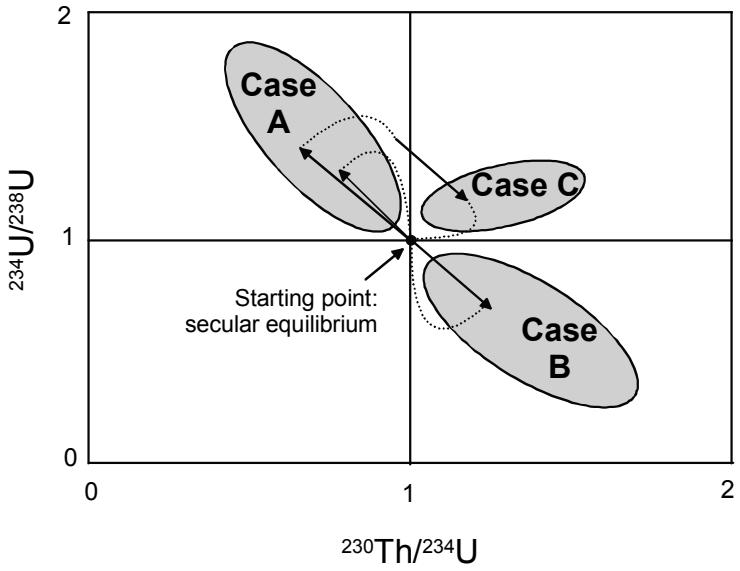

Fig. 6.1: *Effects of disturbed secular equilibrium. Case A: Selective gain of ^{234}U; Case B: Selective loss of ^{234}U; Case C: Combined selective gain and loss of ^{234}U. The activity of ^{230}Th remains constant. This approach is based on the model of preglacial calcite formation.*

6.1.1.1 Selective gain of ^{234}U (Case A)

Fig. 6.2 shows the HRL Äspö samples, which have been measured by means of TIMS and have been corrected for the ^{232}Th-content of the detritus. They are based on the model of preglacial calcite formation and have been disturbed again by ^{234}U-gain after a previous state of secular equilibrium. The ages and the degrees of disturbance for the samples can be worked out either on the basis of the diagram or mathematically.

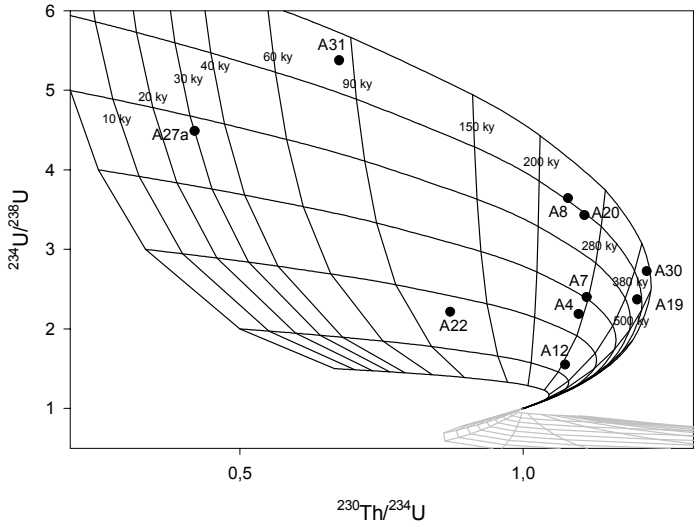

Fig. 6.2: *Activity ratios measured (and corrected) in samples from the HRL Äspö plotted in a $^{234}U/^{238}U$-$^{230}Th/^{234}U$ diagram. These samples have been disturbed by a selective gain in ^{234}U.*

In order to determine the ages and the degrees of disturbance for the samples mathematically, Eqs. 5.1 - 5.3 are converted in such a way that they represent the activities of the isotope in question in each case, which gives the resulting equations (Eq. 6.1-6.3):

$$A(^{238}U) = A(^{238}U_{event}) \cdot e^{-\lambda_{238} t} \qquad \text{(Eq. 6.1)}$$

$$A(^{234}U) = A(^{238}U_{event}) \cdot \frac{\lambda_{234}}{\lambda_{234} - \lambda_{238}} \cdot \left(e^{-\lambda_{238} t} - e^{-\lambda_{234} t}\right) + A(^{234}U_{event}) \cdot e^{-\lambda_{234} t} \qquad \text{(Eq. 6.2)}$$

$$A\left(^{230}Th\right) = A\left(^{238}U_{event}\right)\lambda_{234}\lambda_{230}\left(\frac{e^{-\lambda_{238} t}}{\left(\lambda_{234} - \lambda_{238}\right)\left(\lambda_{230} - \lambda_{238}\right)} + \frac{e^{-\lambda_{234} t}}{\left(\lambda_{238} - \lambda_{234}\right)\left(\lambda_{230} - \lambda_{234}\right)}\right.$$

$$\left. + \frac{e^{-\lambda_{230} t}}{\left(\lambda_{238} - \lambda_{230}\right)\left(\lambda_{234} - \lambda_{230}\right)}\right) + A\left(^{234}U_{event}\right) \cdot \frac{\lambda_{230}}{\lambda_{230} - \lambda_{234}} \cdot \left(e^{-\lambda_{234} t} - e^{-\lambda_{230} t}\right)$$

$$+ A\left(^{230}Th_{event}\right) \cdot e^{-\lambda_{230} t} \qquad \text{(Eq. 6.3)}$$

The equations for the activity ratios of $^{234}U/^{238}U$ and $^{230}Th/^{234}U$ are used to more specifically determine the time t and the degree of disturbance for the samples (Eqs. 6.4 ad 6.5).

$$\frac{A\left(^{234}U\right)}{A\left(^{238}U\right)} = \frac{A\left(^{238}U_{event}\right) \cdot \frac{\lambda_{234}}{\lambda_{234} - \lambda_{238}} \cdot \left(e^{-\lambda_{238} t} - e^{-\lambda_{234} t}\right) + A\left(^{234}U_{event}\right) \cdot e^{-\lambda_{234} t}}{A\left(^{238}U_{event}\right) \cdot e^{-\lambda_{238} t}} \qquad \text{(Eq. 6.4)}$$

$$\frac{A\left(^{230}Th\right)}{A\left(^{234}U\right)} = \frac{A\left(^{238}U_{event}\right)\lambda_{234}\lambda_{230}\left(\frac{e^{-\lambda_{238} t}}{\left(\lambda_{234} - \lambda_{238}\right)\left(\lambda_{230} - \lambda_{238}\right)} + \frac{e^{-\lambda_{234} t}}{\left(\lambda_{238} - \lambda_{234}\right)\left(\lambda_{230} - \lambda_{234}\right)}\right.}{A\left(^{238}U_{event}\right) \cdot \frac{\lambda_{234}}{\lambda_{234} - \lambda_{238}}}$$

$$\frac{\left. + \frac{e^{-\lambda_{230} t}}{\left(\lambda_{238} - \lambda_{230}\right)\left(\lambda_{234} - \lambda_{230}\right)}\right) + A\left(^{234}U_{event}\right) \cdot \frac{\lambda_{230}}{\lambda_{230} - \lambda_{234}} \cdot \left(e^{-\lambda_{234} t} - e^{-\lambda_{230} t}\right)}{\cdot \left(e^{-\lambda_{238} t} - e^{-\lambda_{234} t}\right)}$$

$$\frac{+ A\left(^{230}Th_{event}\right) \cdot e^{-\lambda_{230} t}}{+ A\left(^{234}U_{event}\right) \cdot e^{-\lambda_{234} t}} \qquad \text{(Eq. 6.5)}$$

It is not possible to convert the Eqs. 6.4 and 6.5 in such a way that the age t of the samples can be calculated by simply substituting the $^{234}U/^{238}U$- or $^{230}Th/^{234}U$- activity ratios that have been measured by means of TIMS and subsequently been corrected for detrital Th. Therefore t is determined iteratively, which results in an age value for each the $^{234}U/^{238}U$- and the $^{230}Th/^{234}U$-activity ratio. The two age values are then adjusted to the degree of disturbance of the sample, proceeding iteratively again. The values for the samples from the HRL Äspö thus obtained are shown in Tab. 6.1.

Tab. 6.1: Age and degree of disturbance of selective HRL Äspö samples which have selective gained ^{234}U. The age and degree of disturbance are calculated by Eq. 6.4 and 6.5.

Sample	Age of disturbance	Degree of
A4	269	3.5
A7	276	4.0
A8	230	6.0
A12	287	2.2
A19	436	5.6
A20	253	5.9
A22	118	2.7
A27a	30	4.8
A30	429	6.7
A31	84	6.5

6.1.1.2 Selective loss of 234U (Case B)

Fig. 6.3 represents the samples from the HRL Äspö measured by TIMS which have been redisturbed through loss of ^{234}U after a state of secular equilibrium. The interpretation of these samples are based on the model of preglacial calcite formation, too.

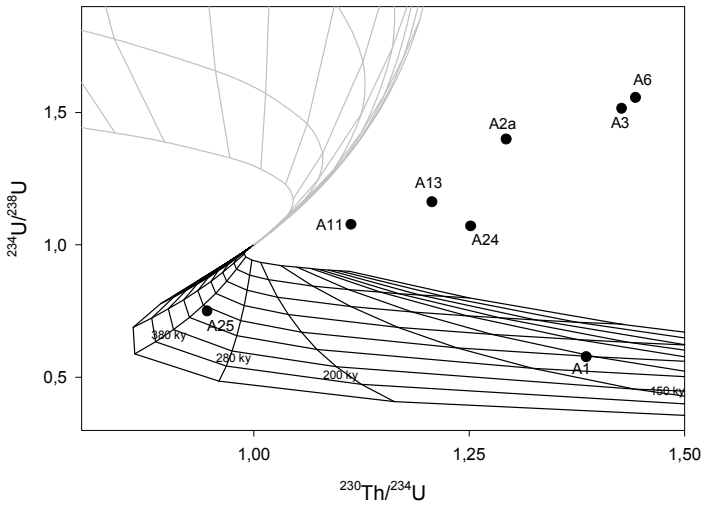

Fig. 6.3: *Activity ratios (corrected for detritus) of fracture minerals from the HRL Äspö. Shown are samples which have been disturbed by selective loss of ^{234}U.*

Fig. 6.3 shows that except for A1 and A25 the samples obviously have not been disturbed through selective loss of ^{234}U in a state of secular equilibrium. This leads to the hypothesis that the samples which have undergone selective loss of ^{234}U and are outside the diagram grid in Fig. 6.3, have been affected by at least two disturbing events since their former state of secular equilibrium. The activity ratios of $^{234}U/^{238}U$ and $^{230}Th/^{234}U$ of these calcites both have a value > 1. This set of samples will be referred to as Case C and be discussed in Chapter 6.1.1.3.

The calculation of both the age and the degree of disturbances for the samples A1 and A25 proceeds along the lines described in Chapter 6.1.1.1. The age of the samples is determined iteratively utilizing Eqs. 6.4 and 6.5, and the two resulting age values are adjusted to the degree of disturbance again by way of iteration. The thus obtained values for the samples A1 and A25 from the HRL Äspö, which have been disturbed in their secular equilibrium through selective loss of ^{234}U, are shown in Tab. 6.2.

Tab. 6.2: Age and degree of disturbance of two samples from the HRL Äspö which selectively have lost ^{234}U. Age and degree of disturbance according to Eq. 6.4 and 6.5 by iteration

Sample	Age of disturbance	Degree of disturbance
A1	64	0.5
A25	257	0.5

6.1.1.3 Combined selective gain and loss of 234U (Case C)

For those samples plotting outside the diagram grid in Fig. 6.3 a combination of two disturbances of the isotope ratios must be assumed. These processes will now be described with the help of the diagrammatic representation in Fig. 6.4. Given that the calcites initially are in a state of secular equilibrium, a disturbance of the isotope ratios by the gain of ^{234}U through a migrating solution is required (Fig. 6.4, Path 2). A closed system ensues for a period of e.g. 500 ky, with the consequence that the calcites develop towards a secular equilibrium again according to the newly emerged $^{234}U/^{238}U$-activity ratio (Fig. 6.4, Path 3). Before the samples achieve the activity ratios $^{234}U/^{238}U = 1$ and $^{230}Th/^{234}U = 1$, they are once more disturbed by a migrating solution, removing ^{234}U from the calcites (Fig. 6.4, Path 4). This explains the formation of the Group C samples.

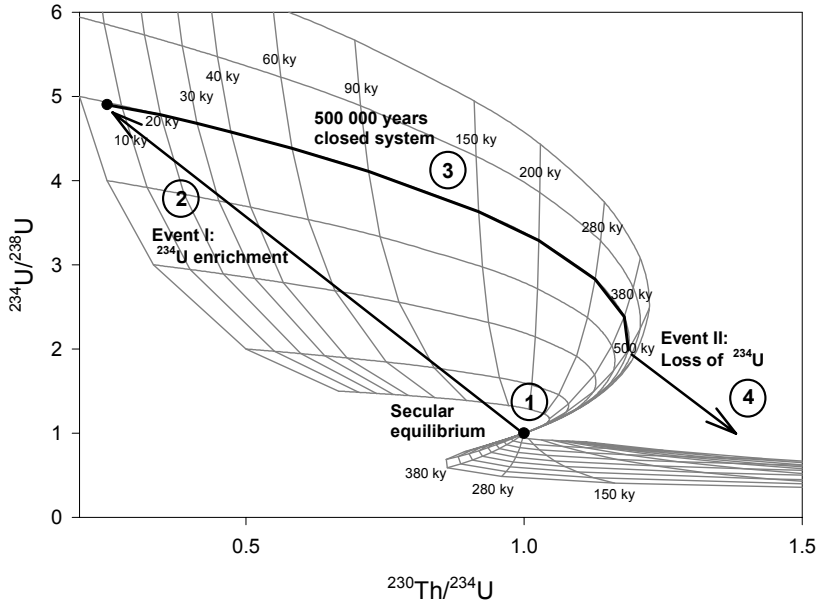

Fig. 6.4: *Principles of activity evolution of samples which have gained ^{234}U and subsequently evolved for a period of 500 ky before a selective loss of ^{234}U occurred in a later event.*

The model for the six Group C samples outlined here is again based on Eq. 5.1 to 5.3. It differs from the model described in Chapter 6.1.1.2 in that the disturbance through migrating underground solutions does not affect a secular equilibrium, but a system that has been closed for ca 500 ky (Fig. 6.5).

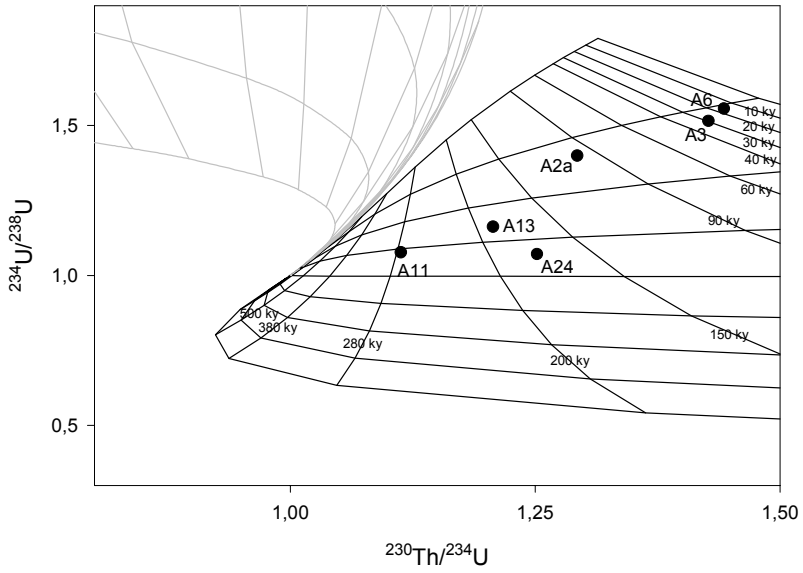

Fig. 6.5: *$^{234}U/^{238}U$-$^{230}Th/^{234}U$ activity ratios of HRL Äspö fracture minerals which have selectively lost ^{234}U after they have developed from an intermediate period of 500 ky which started from a gain in ^{234}U*

For the calculation of the age and the degree of disturbance of the samples the method described in Chapter 6.1.1.1 is applied again. The age of the samples determined iteratively with the Eqs. 6.4 and 6.5 is in turn adjusted to the degree of disturbance by way of iteration. The resulting values for the samples from the HRL Äspö which were disturbed by selective loss of ^{234}U after 500 ky can be taken from Tab. 6.3.

Tab. 6.3: Age and degree of disturbance of samples shown in Fig. 6.5 as calculated from Eq. 6.4 and 6.5 by iteration.

Sample	Age of disturbance	Degree of disturbance
A2a	99	0.8
A3	29	0.8
A6	16	0.8
A11	275	0.6
A13	187	0.6
A24	174	0.6

6.1.2 Model of recently formed calcites

Another theoretical model for the interpretation of the samples investigated here will be discussed next which is based on WALLIN and PETERMAN'S (1999) hypothesis of recently formed fracture minerals in the HRL Äspö during the past 800 ky. The geological conditions lend little support to the model of recent mineral formation, with this study being an isolated case in this respect. Yet, their approach, drawing on the diagram developed by KAUFMAN and BROECKER (1965) which was already discussed in Chapter 5, is a widely used model for the discussion of U/Th-isotope data. Therefore, we will consider the samples from this theoretical angle, too, for the sake of completeness. Two cases (D and E) can be distinguished here.

Case D: With the precipitation of carbonate from an aqueous solution uranium is incorporated in the calcite lattice in the form of a uranyl carbonate complex. Since thorium is little mobile in solutions, the calcite does not take up any significant amount of it. Provided the conditions for a closed system are met and the samples are not affected by migrating underground solutions, the activity ratios of the calcite develop towards a secular equilibrium in the course of time. The current U/Th-isotope ratios thus allows us to draw inferences about the properties of the underground solution. This case will be discussed in Chapter 6.1.2.1.

Case E: If a solution which is undersaturated with $CaCO_3$ meets a calcite of the form described under Case D, it specifically gains ^{234}U, not ^{230}Th or ^{238}U, from the solid, and the isotope ratios of the samples are disturbed. The calcite is left with a deficit of the daughter isotope ^{234}U as a result. After the reaction the activity ratios of the samples develop towards a secular equilibrium again. This case will be discussed in Chapter 6.1.2.2.

6.1.2.1 Primary calcites (Case D)

A diagram following KAUFMAN and BROECKER (1965) is suitable for an account of the undisturbed samples from the HRL Äspö, which are based on the model of recent calcite formation. This model, which has also been applied to the samples from the FL Grimsel, and the equations pertaining to it were described in Chapter 5. Fig. 6.7 shows in a $^{234}U/^{238}U$-$^{230}Th/^{234}U$ activity diagram the samples from the HRL Äspö which have been measured by means of TIMS and have been corrected for the ^{232}Th-content of the detritus.

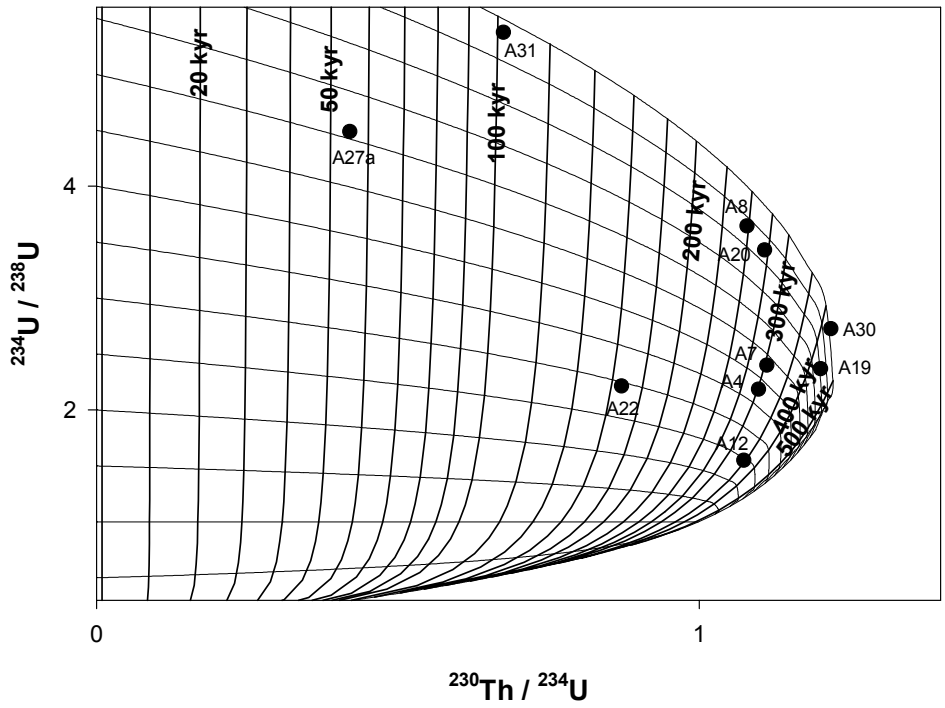

Fig. 6.7: *Conventional isochron diagram according to KAUFMAN und BROECKER (1965). Interpretation of geological ages from this diagram requires the assumption of calcite precipitation from a ^{234}U enriched solution ($^{234}U/^{238}U > 1$)which was not in secular equilibrium. Samples shown are calcites from the HRL Äspö.*

For the undisturbed HRL Äspö samples, which are based on the model of recent calcite formation, the age of formation as well as the initial $^{234}U/^{238}U$-activity ratio are calculated with the Eqs. 5.4 and 5.5. Both values are once more determined iteratively. Substituting the measured and corrected $^{230}Th/^{234}U$-activity ratio in Eq. 5.4 yields the determination of the age. Substituting both the measured and corrected $^{234}U/^{238}U$-activity ratio and the thus determined age in Eq. 5.5 leads to the determination of the initial $^{234}U/^{238}U$-activity ratio of the sample. The values for the HRL Äspö samples obtained in this way are listed in Tab. 6.4. With the model of recently formed calcites serving as the theoretical framework, it shows the real age of formation of the samples.

Tab. 6.4: Calculated age of formation and initial $^{234}U/^{238}U$ activity ratio of calcites from the HRL Äspö. The interpretation of measured activity ratios as ages of formation requires the assumption of calcite precipitation from migrating underground solutions.

Sample	Age of precipitation	$(^{234}U/^{238}U)_{initial}$
A4	301	3.8
A7	31	4.4
A8	248	6.3
A12	345	2.5
A19	445	5.8
A20	270	6.2
A22	166	2.9
A27a	55	5.1
A30	435	6.9
A31	102	6.8

It should be noted here that the $^{234}U/^{238}U$ activity ratios observed in three samples of current underground water vary between 3.9 and 4.5 (see Tab. 4.5). Thus, a wider range of $^{234}U/^{238}U$ activity ratios is requested for those underground solutions from which calcites could have been precipitated during the last 500 ky within the currently accessible HRL tunnel volume.

6.1.2.2 Primary calcites with selective loss of 234U (Case E)

Case E, based on the model of recently formed calcites, comprises the samples from the HRL Äspö whose isotope ratios have been disturbed through selective loss of ^{234}U in their development towards a secular equilibrium. Once again, in close parallel to the calcites in Cases B and C these samples are interpreted within the model especially set up for the loss of ^{234}U, which makes crucial use of Eqs. 5.1 to 5.3. This model differs from the one described in Chapter 6.1.1.2 in that it is based on different assumptions about the age of the formation of the samples.

While the hypothesis put forward in Chapter 6.1.1.2 is that the calcites discussed there were formed preglacially and thus a secular equilibrium existed before the disturbance, the geological conditions in the case of recently formed calcites strongly suggest that the disturbance of their isotope ratios occurred earlier than the disturbance of samples in secular equilibrium. We will assume that the calcites' selective loss of ^{234}U took place 500 ky after their formation. Additional assumptions will be carried over from the model discussed in Chapter 5, which means that e.g. 5 ppm U with an initial $^{234}U/^{238}U$-activity ratio of 5 was incorporated during the formation of the calcites. With this assumption, a model is developed based on the Eqs. 5.1 to 5.3. The diagram that forms the right-hand part of Fig. 6.8 represents a loss of ^{234}U ranging between 10 and 90 per cent, the pertaining isochrons, and the samples from the HRL Äspö which have been disturbed in their development towards a secular equilibrium by a loss of ^{234}U.

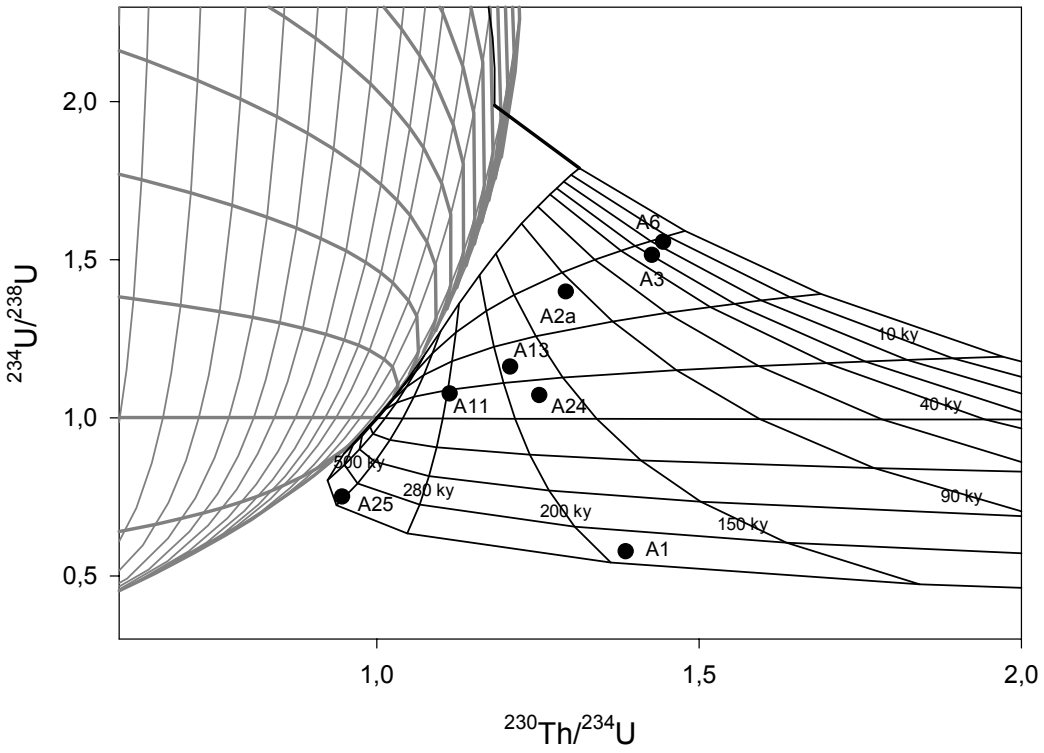

Fig. 6.8: *Activity ratios of samples from the HRL Äspö (corrected for detrital 232Th) plotted in a 234U/238U-230Th/234U diagram. Calculated ages require the assumption of selective loss of 234U 500 ky after their primary precipitation.*

The calculation of the ages and degrees of disturbance proceeds along the same lines as described in Chapter 6.1.1.1. The ages of disturbance for the calcites are first determined iteratively using Eqs. 6.4 and 6.5. Then both the resulting ages are iteratively adjusted to the degree of disturbance. The thus determined values for the samples from the HRL Äspö, which are based on the model of recent calcite formation, are listed in Tab. 6.5.

Tab. 6.5: Age and degree of disturbance of calcites from the HRL Äspö as plotted in Fig. 6.8

Sample	Age of disturbance	Degree of
A1	192	0.1
A2a	99	0.8
A3	29	0.8
A6	16	0.8
A11	275	0.6
A13	187	0.6
A24	174	0.6
A25	386	0.1

6.2 Samples from the FL Grimsel

6.2.1 Model of solid-solid-reactions

6.2.1.1 Selective gain of 234U and loss of 230Th (Case F)

Fig. 6.9 shows the TIMS-measured samples from the FL Grimsel whose isotope ratios were disturbed after a state of secular equilibrium by solid-solid-reactions with the wall rock triggered by α-recoil-effects through a gain of ^{234}U and a loss of ^{230}Th.

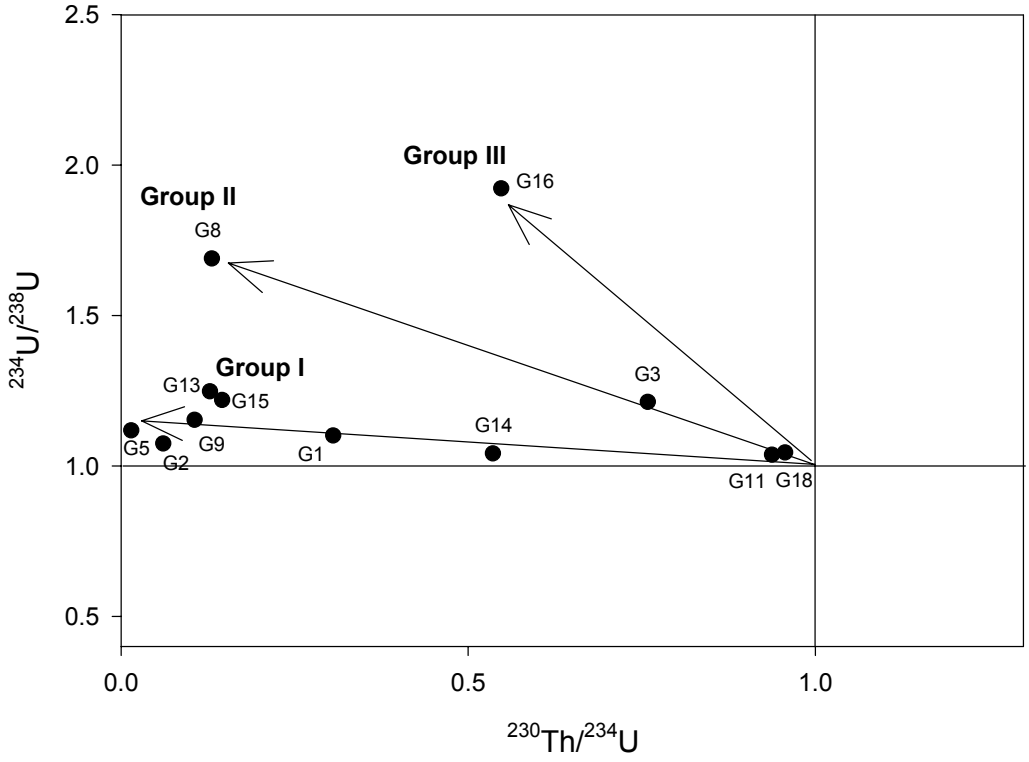

Fig. 6.9: *Sample groups I to III from the FL Grimsel plotted in a $^{234}U/^{238}U$-$^{230}Th/^{234}U$ activity diagram. All samples plotted have $^{230}Th/^{234}U$ activity ratios<1 and are characterized by lower U contents relative to the rock.*

For the fracture mineral samples plotted in Fig. 6.9 the model discussed in Chapter 5 assumes a uranium content higher than that of the neighbouring rock. Assuming 6 ppm in the neighbouring granite and the uranium concentrations of the fracture minerals shown in Tab. A5 of the Appendix of GERDES (2000) this prediction is confirmed with the exception of samples G15 and G5. The arrows in Fig. 6.9 indicate three groups of samples, each with different ratios of ^{234}U gain and ^{230}Th loss. The inspection of the isotope ratios of the fracture minerals in Group I with the samples G1, G2, G5, G9, G13, G14, and G15 in Fig. 6.9 shows that they have lost a lot of ^{230}Th and gained relatively little ^{234}U compared with the other groups. We find a different picture for sample G16 (Group III), whose secular equilibrium has almost exclusively been

disturbed through a gain of ^{234}U. Group II, which includes the samples G3, G8, G11 and G18, takes up an intermediate position with respect to the relation of U-gain and Th-loss. It should be pointed out here again that under this approach to the discussion of the data a system within the rock assemblages must be assumed to be open to changes in isotope ratios, which means that it is not possible to determine any ages of formation or reformation.

6.2.1.2 Selective loss of 234U and gain of 230Th (Case G)

Fig. 6.10 shows the TIMS-measured samples from the FL Grimsel whose isotope ratios were disturbed after a state of secular equilibrium by solid-solid-reactions with the wall rock triggered by α-recoil-effects through a loss of ^{234}U and a gain of ^{230}Th.

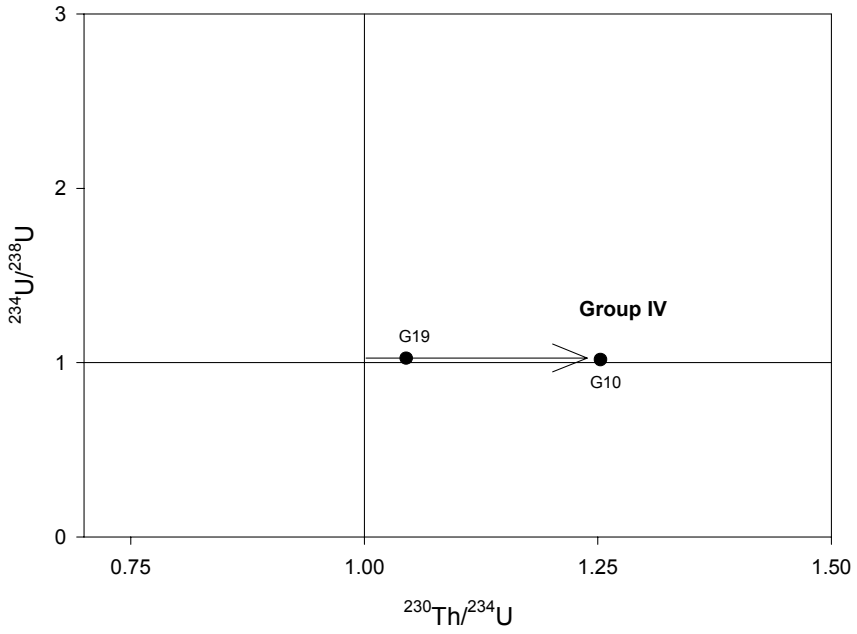

Fig. 6.10: *$^{234}U/^{238}U$-$^{230}Th/^{234}U$ activity diagram for two additional samples from the FL Grimsel with $^{230}Th/^{234}U$ activity ratios > 1 and higher U contents relative to the rock matrix.*

The prediction of the model that the uranium content of the samples in Fig. 6.10 must be higher than that of the wall rock is fulfilled in sample G10 with a content of 10.6 ppm U. The arrow indicates that the two samples only gained ^{230}Th during the disturbance so that they can be assigned to one group with similar isotope evolutions (Group IV). For these samples as well a system within the rock assemblage is assumed to be open to changes in the isotope ratios.

The vein minerals G10 and G19 were adjacent to other samples in the tunnel of the FL Grimsel in each case (G10 adjacent to G11 and G19 to G18). Since the samples G11 and G18 are both members of Group II (^{234}U-gain and ^{230}Th-loss), it is highly improbable that a different behaviour of the wall rock can be observed in so narrow a space. Furthermore, keeping in line with the discussion of Case B in Chapter 5, a loss of ^{234}U would have to be expected for samples G10 and G19 in addition to the gain of ^{230}Th. Since there is obviously no loss of the U-isotope in this case, the model discussed here cannot explain the isotope evolution of these two samples. It should therefore be noted that this model, which is based on the assumption of a system within the granite matrix that is open to changes in the isotope ratios, goes some way towards establishing an explanatory framework; yet, it cannot be applied to all samples from the FL Grimsel.

6.2.2 Model of solid-solution-reactions

For the interpretation of the samples from the FL Grimsel which are based on the model of a closed fracture system with respect to the isotope ratios, the ^{234}U/^{238}U-^{230}Th/^{234}U activity diagram is used according to KAUFMAN and BROECKER (1965) despite the fact that these do not involve the new formation of minerals alone. This way a rough estimate of the ages of the fracture fillings is possible even if they have been altered through their mixing with silicate minerals. The equations used here were discussed in Chapter 5. Fig. 6.11 shows the samples from the FL Grimsel in a ^{234}U/^{238}U-^{230}Th/^{234}U activity diagram. The different symbols represent the different composition of the minerals.

The age and the initial ^{234}U/^{238}U-activity ratio of the samples presently discussed can be calculated similarly to those of the recently formed calcites from the HRL Äspö. On the assumption of the recent formation of these minerals the resulting age would be their real age of formation. The mixture of calcitic and silicate components in most of the samples, however, suggests that these ages can only be interpreted as maximum ages. They will only be determined and discussed in the case of recently formed calcites.

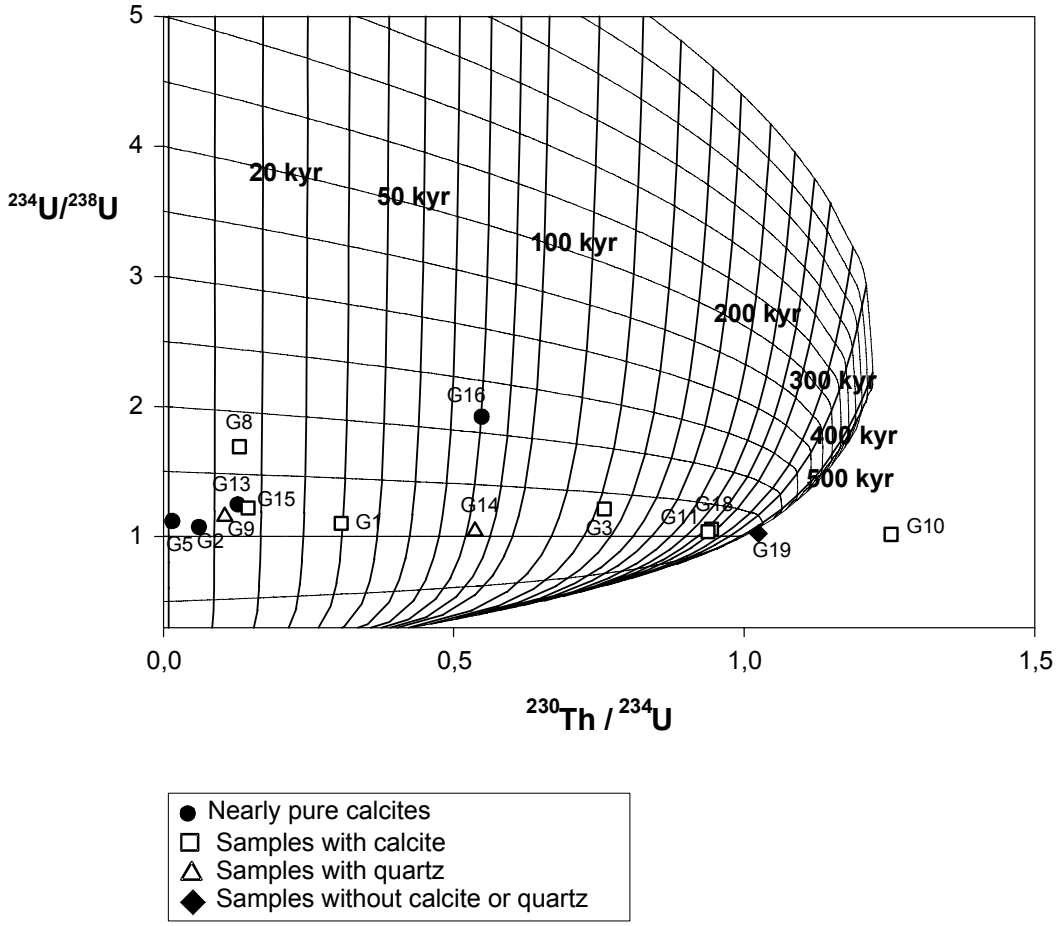

Fig. 6.11: *Conventional $^{234}U/^{238}U$-$^{230}Th/^{234}U$ isochron plot according to KAUFMAN und BROECKER (1965). Application of this diagram assumes a closed-system evolution of fracture mineral assemblages from the FL Grimsel (see text for further explanation).*

The samples have been divided up into four groups according to their mineral components:

- nearly pure calcites (G2, G5, G13 and G16),
- calcite-bearing samples (G1, G3, G8, G10, G11 and G18),
- quartz-bearing samples (G9 and G14), and finally
- samples without any calcite or quartz (G19) (cf. Fig. 6.11).

All these groups are supposed to be instances of complex mixtures ranging from an unaltered pure silicate composition to nearly pure calcites. The limiting members of this scale are the group of nearly pure calcites as new formations at the one extreme and the group of samples free of calcite and quartz at the other. The isotope ratios of the samples involving mixtures with an intermediate position on the scale are influenced by both limiting members. The more recently formed minerals a sample contains, the more it will be shifted from the state of secular equilibrium towards the left side of the diagram in Fig. 6.11. In addition to calcite we also take the formation of low-quartz from an aqueous solution (e.g. TRÖGER 1967) to be a recent formation, which can widely be found as a fracture filling.

Since the samples grouped as relatively pure calcites are real new formations, their age and initial activity ratio must be determined here. The age is the result of applying Eq. 5.4 and the value measured for the $^{234}U/^{238}U$-activity ratio of the sample. The initial $^{234}U/^{238}U$-activity ratio in Eq. 5.5 is calculated by means of the measured $^{234}U/^{238}U$-activity ratio and the previously established age. The data for the pure calcites from the FL Grimsel resulting from this calculation are summed up in Tab. 6.6.

Tab. 6.6: Calculated age of formation and initial $^{234}U/^{238}U$ activity ratio of four calcite-dominated samples from the FL Grimsel. The age of formation and the initial $^{234}U/^{238}U$-have been derived by application of Eq 5.4 und 5.5 by iteration.

Sample	Calculated age of formation	$(^{234}U/^{238}U)_{initi}$
G2	7	1.1
G5	2	1.1
G13	15	1.3
G16	80	2.1

The samples G2, G5 and G13 will be classified here as one group with respect to their age. Thus the migration of an aqueous, $CaCO_3$-saturated solution 2 ky up to 15 ky ago would qualify as the most recent event in the FL Grimsel. Since such young ages can only be obtained with an error margin of 20 %, these figures will be interpreted as a clue to recent formations. On account of sample G16 a further intrusion of a solution into the FL Grimsel can be assumed to have taken place about 80 ky ago.

Sample G19 is the second limiting member of the scale of fracture fillings analyzed here. Fig. 6.11 shows that the isotope ratios of the sample are approximately in a state of secular equilibrium, which suggests a very old formation age of the sample. The only visible deviation of the activity ratios $^{234}U/^{238}U$ and $^{230}Th/^{234}U$ from 1 is due to a small loss of ^{234}U. This can be explained through a ^{234}U-loss of the silicate mineral to a migrating solution, as already described in Chapter 5.

For the fracture fillings which consist of a mixture of newly formed and old minerals, the determination of the formation age is not possible. It is conceivable that the amount of newly formed minerals in the samples has the age of the pure calcites and thus was formed recently or 80 ky ago. The assumption that the newly formed components in all samples have the same age would appear to allow statements about the mixing ratio of new and old minerals for each sample. The sample G15, for instance, comes from the same site as the fracture minerals G2 and G5, which were formed under recent conditions. It therefore seems likely that the newly formed component of this sample is of recent origin as well, while the isotope ratios have been slightly changed by the silicate component. Since it is unclear, however, whether the relevant event for each sample occurred recently, 80 ky ago or at another time, these estimates are questionable. The only sample that cannot be explained by this model is sample G10, which is outside the range between the two limiting members. While it seems plausible that the silicate component of this sample which is marked by a particularly great ^{234}U-loss has considerable influence on the isotope ratios, it still remains unclear why none of the other samples are affected by such a severe disturbance of the ^{234}U-amount.

7 Spatial and temporal distribution of U/Th disequilibria

7.1 Samples from the HRL Äspö

The location of samples from the HRL Äspö is crucial in further discussing of the age and the degree of disturbance of the samples. Fig. 7.1 is a simplified plan of a tunnel section in the HRL Äspö with the sampling sites of the calcites measured here. Sample A31 was taken in a part of the tunnel further to the north and is therefore not included in Fig. 7.1. The model of preglacially formed calcites will be discussed first.

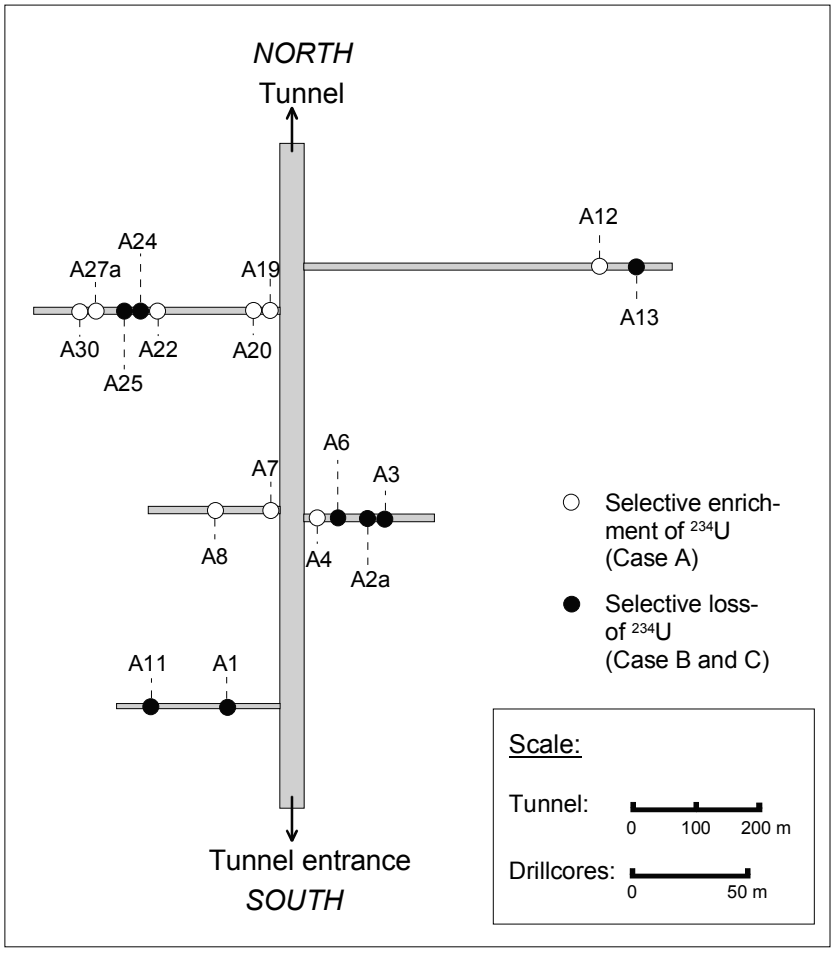

Fig. 7.1: *Schematic sketch of a tunnel section of the HRL Äspö showing the sites of fracture mineral sampling. Open symbols represent samples which selectively have gained ^{234}U, filled symbols represent samples which have experienced a selective loss of ^{234}U. Note the different scales for tunnel meters and drill core meters.*

The open dots in Figs. 7.1 to 7.3 represent positions of samples which selectively gained ^{234}U during the migration of underground solutions and whose secular equilibrium has been disturbed as a result (Case A). Calcite samples which underwent loss of ^{234}U out of a state of equilibrium are marked by filled dots (Case B). The Case C samples will here be considered together with the calcites of Case B, because their last datable disturbance was a selective loss of ^{234}U, too. Note the different length scales for the tunnel and the drill cores in Figs. 7.1 to 7.4; the scale for the drill cores has been enlarged by about a factor of 4 to ensure a clear representation of the samples in the tunnel.

Consideration of the samples' degree and age of disturbance with respect to their sites (see Figs. 7.2 and 7.3) provides a basis for hypotheses about the course of events disturbing the isotope ratios of the samples. Degrees of disturbance < 1 indicate that a migrating solution removed ^{234}U from the calcite. Samples with a degree > 1 represent the case of a solution adding ^{234}U to the calcite. Grouping the samples marked by open dots diagramatically (the hatched area in Fig. 7.2) shows that those disturbances of a secular equilibrium that involve gain of ^{234}U are predominantly located along a hypothetical NE-SW-axis, which corresponds to the main direction of some currently observed fracture systems within the tunnel.

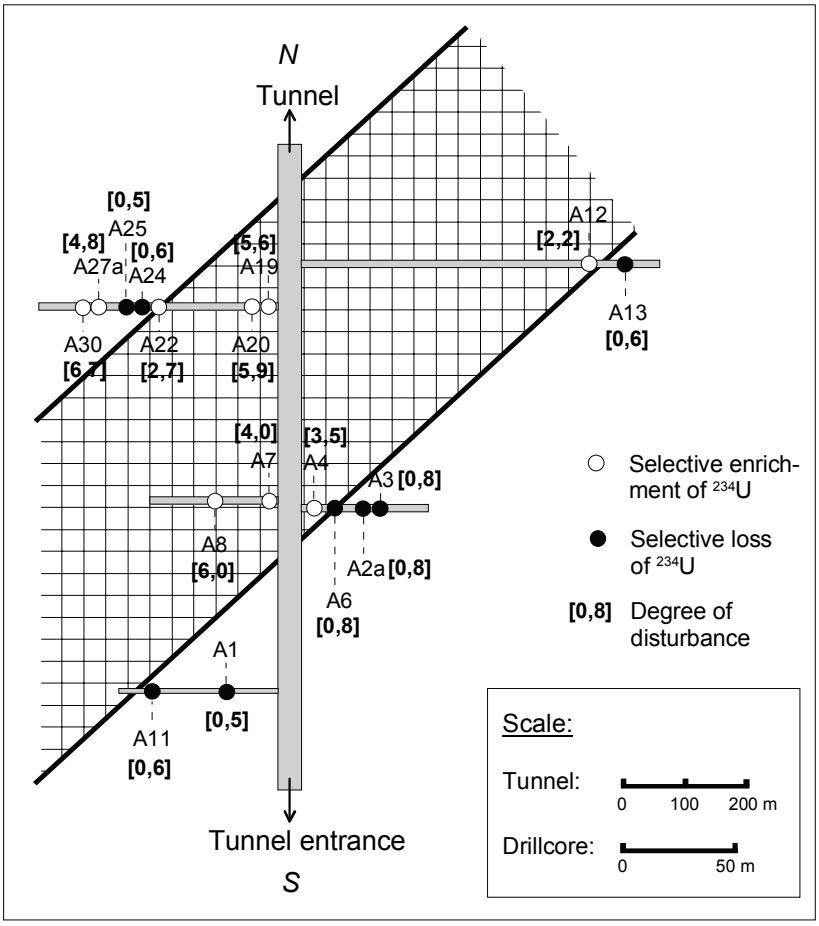

Fig. 7.2: *Schematic sketch of a tunnel section of the HRL Äspö showing the sampling sites. Figures plotted adjacent to the sample numbers represent the degrees of disturbance.*

As to the area with an NE-SW trend that shows selective gain of ^{234}U (hatched area in Fig. 7.2), we observe that the peripheral fracture samples exhibit lower degrees of disturbance than the more central samples. Examples are sample A12 at the periphery of the marked area with the low disturbance value 2.2, and sample A8, which on account of its value of 6.0 occupies a more central position with selective gain of ^{234}U.

A possible explanation is the hypothesis that there have been different generations of underground solutions with different ^{234}U-concentrations migrating through the granite from NE to SW, whereby the calcites have undergone varying degrees of enrichment of ^{234}U. On the other hand, it is observed that degrees of disturbance have a tendency to increase perpendicularly to the NW-SE axis within the area of samples with selective ^{234}U-gain. A plausible alternative hypothesis therefore is that a solution containing excess ^{234}U entered the granite along the main fracture system's NE-SW direction (see Fig. 7.3, where this direction has been termed 'Axis of disturbance').

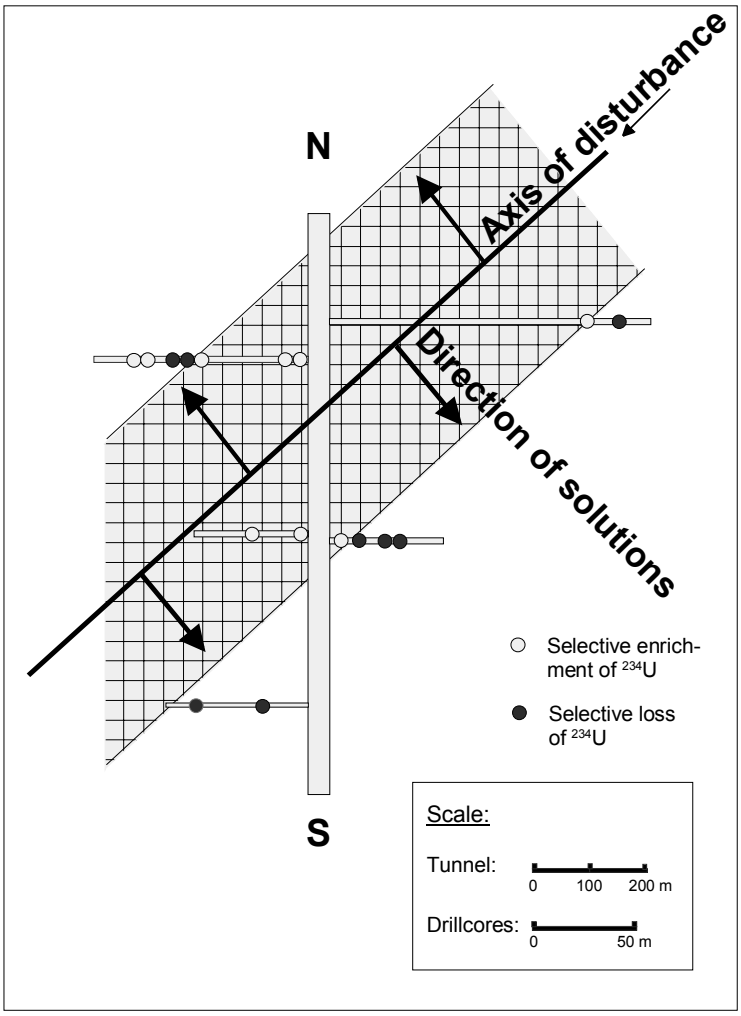

Fig. 7.3: *Schematic sketch of assumed migration fronts within the HRL tunnel section shown in Fig. 7.2.*

The secular equilibrium of the calcites closest to the fracture was disturbed and the samples were enriched with ^{234}U in large amounts, a high degree of disturbance being the consequence. As the solution reacted with other calcites it was gradually deprived of ^{234}U with its progressing migration through the granite (Fig. 7.3, where this has been termed 'Direction of solutions'). The effect of this was that the solution disturbed the secular equilibrium of the calcites in neighbouring fracture systems less strongly and that the enrichment of ^{234}U was not that high. Thus we have lower values for the disturbance degrees at the periphery of the area with selective ^{234}U-gain.

Both south and north of the hatched area in the diagram calcite fracture fillings have been found which underwent selective loss of ^{234}U. Their values for the degree of disturbance range from 0.1 to 0.8. Combining this finding with the assumption that the solution migrating through the rock is more and more deprived of ^{234}U during its migration through the hatched area in the diagram, it is quite conceivable that the very same solution has disturbed the samples north and south of this area as well.

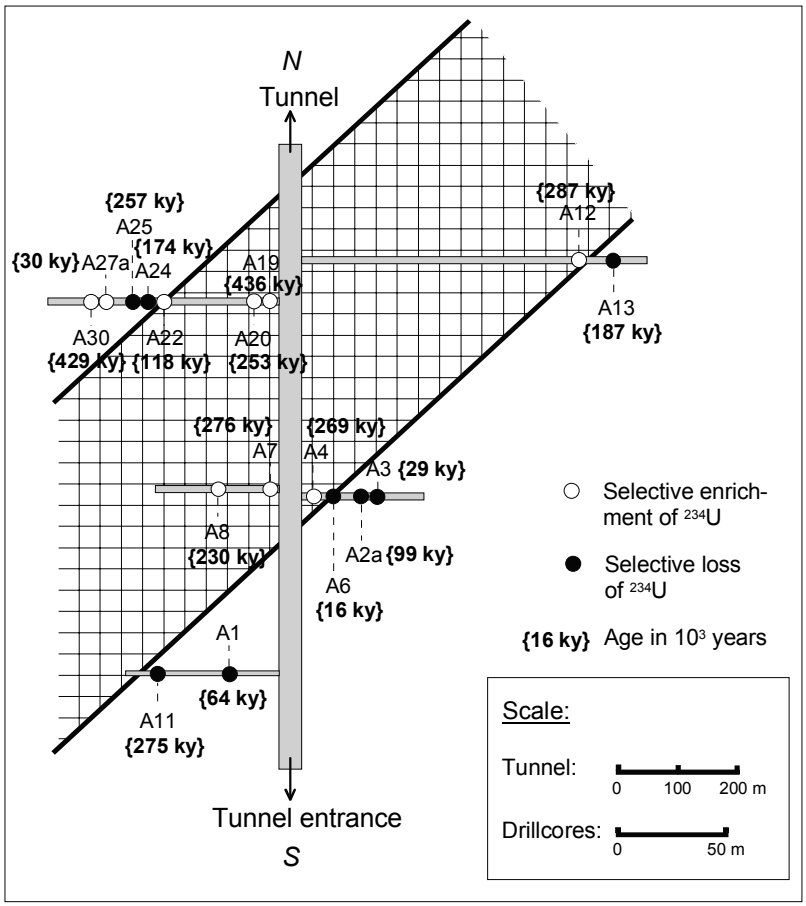

Fig. 7.4: *Schematic sketch of a HRL tunnel section HRL Äspö showing the sites of sampling fracture fillings along with the calculated ages of disturbance (ky).*

Fig. 7.4 represents the time passed since the last hydrothermal disturbance of the samples by also linking it to their sites in the tunnel.

Similarly to what was observed in the discussion of the disturbance degrees, some calcites, too, show a trend of their development in their positions in the tunnel with respect to their disturbance ages. It can be seen that within the NE-SW-oriented area with selective ^{234}U-gain the oldest ages tend to be in the middle, e.g. 436 ky for sample A19; younger ages are to be found at the periphery of the inner zone, e.g. 118 ky for sample A22.

This lends support to the idea of a slowly migrating solution front perpendicular to the assumed NW-SE-axis which disturbed the secular equilibria of the calcites over a period of several tens of thousands of years for the samples within the hatched area. In those areas that contain samples with a selective loss of ^{234}U (marked by black dots) no correlation can be recognized between the ages and the locations of the samples. The same solution probably has disturbed the isotope ratios of both the samples characterized by ^{234}U-gain and those displaying ^{234}U-loss cannot be confirmed.

It is a more plausible hypothesis that the isotope ratios of the two sets of samples have been disturbed by different underground solutions independent of each other. Furthermore, in the region south of the hatched area not even a temporal development can be made out with respect to the disturbance of the secular equilibrium in an NE-SW-direction. It thus seems a safe assumption that the samples in this area have been influenced by solutions from more than one fracture system.

Looking at these facts in comparison to those established in the context of the model of recently formed calcites a comparison can be made of the ages of disturbance and formation on the one hand and of the degrees of disturbance and initial $^{234}U/^{238}U$-activity ratios on the other. Tab. 7.1 shows that the data derived from preglacial or recent formation conditions are consistently different from each other with only a few exceptions (predominantly with young ages, A1, A27a). Therefore, detailed analyses of the data established under the model of recent calcite formations are not given with respect to their correlation with the location of the relevant samples in the HRL Äspö.

Tab. 7.1: Calculated age of disturbance versus age of formation and calculated degree of disturbance versus $^{234}U/^{238}U$ initial ratios of samples from the HRL Äspö. The two respective sets of data are related to the model of either 'preglacial' formation or 'recent' formation, respectively. For further comments see text.

Sample	Age of disturbance/age of formation		Degree of disturbance / $(^{234}U/^{238}U)_{initial}$	
	'Preglacial' formation	'Recent'	'Preglacial' formation	'Recent' Formation
A1	64	192	0.5	0.1
A2a	99	99	0.8	0.8
A3	29	29	0.8	0.8
A4	269	301	3.5	3.8
A6	16	16	0.8	0.8
A7	276	317	4.0	4.4
A8	230	248	6.0	6.3
A11	275	275	0.6	0.6
A12	287	345	2.2	2.5
A13	187	187	0.6	0.6
A19	436	445	5.6	5.8
A20	253	270	5.9	6.2
A22	118	166	2.7	2.9
A24	174	174	0.6	0.6
A25	257	386	0.5	0.1
A27a	30	55	4.8	5.1
A30	429	435	6.7	6.9
A31	84	102	6.5	6.8

The models of either the preglacial or recent formation conditions for the calcites are plausible approaches to the analysis of the samples from the HRL Äspö. It should be noted, however, that for the processes claimed in either of these models it cannot be the case that they have taken place simultaneously. Yet, both models have in common that they share the mobilization of uranium through migrating solutions in the past 16 ky to 450 ky.

7.2 Samples from the FL Grimsel

The models described in Chapter 5, both of which are based on a late alpidic formation of the fracture fillings following the geological framework of KEUSEN et al. (1989), are open to different conclusions. In the first model the neighbouring rock assemblages are assumed to be an open system, which makes the dating of the minerals impossible. As a consequence, a dependency relation between their sites in the rock laboratory and the temporal development of the disturbance cannot be established either. The only disturbance-related grouping of samples found in this model is based on the relation between loss and gain of ^{234}U and ^{230}Th (Groups I, II, III, and IV). Fig. 7.5 shows the sites of the samples in the FL Grimsel and the groups they are assigned to (designated by roman numerals).

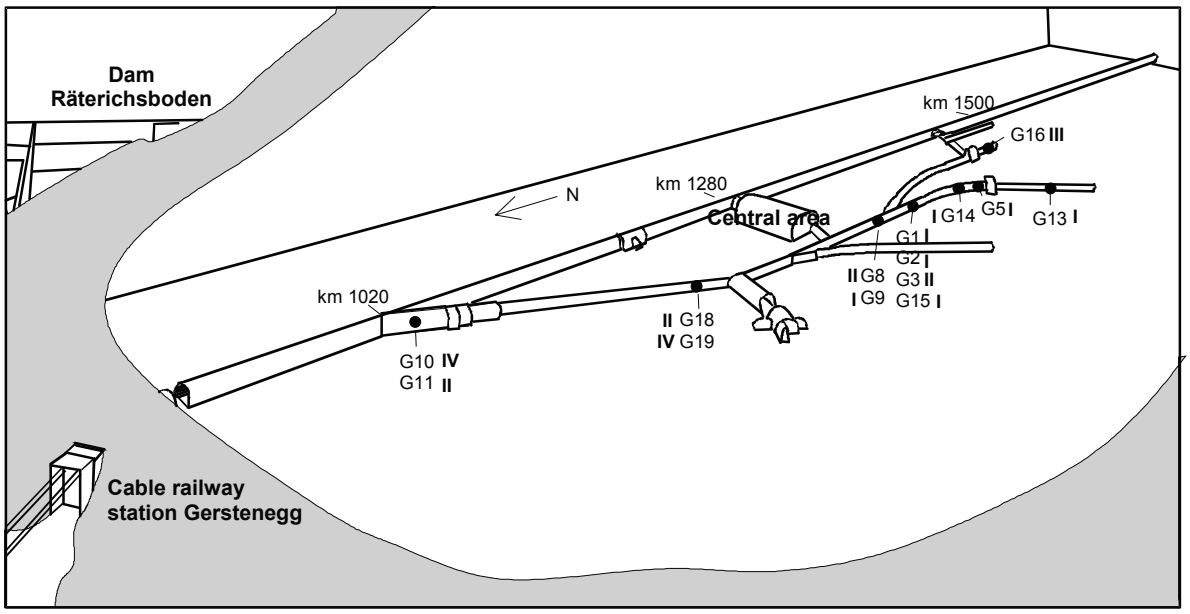

Fig. 7.5: *Subvertical sketch of the FL Grimsel showing sampling sites of fracture minerals. Numbers I to IV refer to groups of fracture minerals according to their modes of formation.*

The samples G1, G2, G5, G9, G13, G14 and G15 can all be brought together in Group I, because they lost ^{230}Th and gained ^{234}U to largely the same extent during their disturbance. The problem with such grouping, however, is that one does not recognize a uniform relationship between this fact and the sites of these samples. While the Group I fracture fillings G1, G2 and G15 were all sampled at one and the same site in the FL Grimsel, the model still does not explain why sample G3 with the same local origin deviates from this categorization in that it is to be assigned to Group II. The samples G10 and G19 illustrate a similar case. These two fracture minerals are the only samples analyzed in this study that have gained the isotope ^{230}Th. Yet, their sites are right next to those of the samples G11 and G18 (both members of Group II), which have lost ^{230}Th. Since it is highly improbable that two completely different types of disturbance of the isotope ratios would occur in so small an area, this model with its firm roots in the geology described in the literature might be used as a basic approach towards a solution of the problems at hand, the conclusions based on it must be treated with caution, though.

The second model that has been proposed for the samples from the FL Grimsel claims that there is a closed vein system. Here the true age of most of the samples has been altered by the influence of a silicate component. As a consequence, the ages of formation or disturbance for all these samples in relation to their sites in the FL Grimsel cannot be discussed here either. Only for the pure calcites could two events be dated as ca. 8 ky (G2, G5 and G13) and 80 ky (G 6) ago. Although it is not unlikely that the newly formed mineral components of all the other fracture fillings was also precipitated at one of these two times, the mixing ratio between the calcitic and the silicate components of the samples is unknown, which makes further estimates impossible. Contrary to positions held in the relevant literature (e.g. KEUSEN et al. (1989)), not only old fracture fillings in secular equilibrium but also recent mineral formations in the FL Grimsel can be identified with this model.

8 Summary and conclusions

In this study the U/Th-isotopes of fracture fillings from granites have been analyzed in order to show the principles of actinide mobility during water-rock interactions in the geological past, i.e. over the past 500 ky. In particular, a method has been developed for the interpretation of U/Th-isotope data which traditional approaches cannot explain. For the calcites from the HRL Äspö and the fracture minerals from the FL Grimsel a number of interpretation models including their mathematical approaches have been developed which differ in the basic geological conditions they assume.

Two models for the explanation of non equilibrium $^{230}Th/^{234}U$ and $^{234}U/^{238}U$ activity ratios have been developed: *i*) a recent formation of fracture minerals (mainly calcites) from underground aqueous solutions and *ii*) the isotopic disturbance of fracture minerals that formed before the last glaciation.

i) The model of the recent formation of calcites from Äspö granitoids is based on the hypothesis that minerals have been newly formed by $CaCO_3$-saturated solutions in the last 800 ky. However, this model of calcite formation appears to be rather improbable, given the hydrogeochemical characteristics of glacial waters. There is only one study in the literature (WALLIN and PETERMAN, 1999) that argues for a formation of calcites in the past glacial periods; all the other authors assume a much older age for the vein minerals.

ii) The model of the preglacial formation of calcites in Äspö granitoids claims a pre-existing secular equilibrium of the minerals and a subsequent disturbance of the isotope ratios by a solution migrating through the granitic rock. Disturbance ages from 20 ky up to 400 ky can be found here, which correlate with the sampling sites of the calcites within the HRL tunnel volume.

There is still one aspect on which the two models *i*) and *ii*) converge: the mobilization of U by migrating solutions in the past 400 ky, independent of the model of older or recent fracture minerals.

For the HRL Äspö with its extensive availability of underground water, a distinct mobility of ^{234}U and ^{238}U over the past 500 ky is manifested in calcite fracture fillings which have reacted with such solutions. The spatial distribution of isotopic disequilibria within a single sampling area outlines the effects of solution-fracture-interaction within a zone that has been affected by one or more generations of migrating underground solutions. Summarizing the insights derived from the isotopic ratios of U and Th in fracture minerals of the FL Grimsel and the HRL Äspö it is concluded that one of the limiting factors of actinide migration through open or partly filled fractures is the availability of underground water. The absolute mass of U being transported during this time span remains unknown but is expected to be small in comparison with the total amount of natural U contained in the granitic rock. The long-term availability of migrating underground solutions has (repeatedly) disturbed the short live U-decay products and has prevented a complete sorption of U by the rock matrix.

In the FL Grimsel, the currently observed hydraulic systems differ from that of the HRL Äspö, in that the flux of underground solution through fracture systems is by orders of magnitude higher in the latter. On the assumption that this principal difference has been maintained for the last 500 ky, it can be concluded that the isotopic disturbances of the Grimsel fracture minerals have been more or less accidental with an emphasis on solid-solid- reactions causing U/Th isotope disequilibria. Thus, the amount of U transported in underground solutions over the past 500 ky is less pronounced than that supposed for the HRL Äspö.

As for the question of a final disposal of radioactive waste in the granite host rocks, the migration in open-system underground solutions of at least uranium - and thus of the similarly behaving actinides - in the near geological future, *i.e.* the next 500 ky can therefore not be ruled out. The production of U/Th isotopic anomalies and thus the mobility of uranium obviously depends on the availability of underground solutions in the rock volumes envisaged for canisters emplacement. In case of a failure of the technical barrier, any Np or Pu leaving the canister - along with U - is expected to be mobile for time spans > 10 ky in the same way as U was mobile during the geological past. Thus, the continuous availability of underground water is regarded in this context as a disadvantage for granites containing large water-bearing fracture zones. If the case of canister failure is included in a safety scenario for a HAW repository, granitic rocks with large open fracture systems, which have connections to the biosphere should be regarded with precaution. With respect to actinide mobility in underground solutions, rock volumes should be selected - if ever possible - which are unfractured and which reveal a minimum access to migrating underground solutions.

The current study of U/Th isotopes in the HRL Äspö is based on a rather limited number of samples originating from a rather small volume of granite. The study may serve as a first step towards further investigation of U/Th isotopic equilibria in a more extended volume of Äspö granitoids in that it presents a set of examples for exploiting the spatial and temporal information which are fixed in fracture minerals. In addition, the study has worked out the methodical principles of interpreting complex isotope signatures for the short-lived daughters down to ^{230}Th which may serve as tools for further projects dealing with U/Th isotopes as natural analogues for actinides in granitic rocks.

9 Acknowledgements

This project was undertaken as part of a research scheme funded by the *Bundesministerium für Wirtschaft (BMWi)*. The PtWT+E at the *Forschungszentrum Karlsruhe* kindly took care of its organizational side. The continuous and constructive support by Werner Bechthold (PtWT+E) is gratefully acknowledged. This work would not have been possible without the generous assistance of the SKB staff at the Äspö Hard Rock Laboratory. We are especially indebted to Olle Olsen, Mansueto Morosini and Leif Stenberg for their help in organizing and carrying out field work and various underground activities. As to the FL Grimsel, special thanks go to Toni Bär (NAGRA) and Herbert Kull (GRS Braunschweig) for generous support in the sampling campaigns. The analyses of U/Th isotope ratios of fracture minerals by Prof. A. Mangini (Heidelberg University) and Prof. A. Eisenhauer (GEOMAR, Kiel) also is gratefully acknowledged.

Thanks are also due to the staff of the Department of Mineralogy, Geochemistry and Salt Deposits at the TU Clausthal: Kai Schmidt for trace element analyses by means of ICP-MS, and Michael G. Siemann for his help with XRD-analyses and for constructive criticism and fruitful discussions throughout the course of the project.

10 References

ABRECHT, J., SCHALTEGGER, U. (1988): Aplitic intrusions in the Central Aar massif basement: Geology, petrography and Rb/Sr data. Eclogae geologicae Helvetiae 81: 227-239.

BATEMAN, H. (1910): Solution of a system of differential equations occurring in the theory of radioactive transformations. Proceedings Cambridge Philosophical Society 15: 423-427.

BOLLHÖFER, A. (1996): Uranreihen-Datierung diagenetischer Manganknollen mittels Thermionen-Massenspektrometrie (TIMS): klimainduzierte Wachstumsschwan-kungen im Spätquartär. Dissertation, Ruprecht-Karls-Universität Heidelberg,

CHEN, J.H., EDWARDS, L.R., WASSERBURG, G.J. (1986): ^{238}U, ^{234}U and ^{232}Th in sea water. Earth and Planetary Science Letters, 80: 241-251.

CHERDYNTSEV, V.V. (1971): Uranium-234. Israel program for Scientific translations.

DICKIN, A.P. (1995): Radiogenic isotope geology. Cambridge University Press.

FAURE, G. (1986): Principles of isotope geology. John Wiley & Sons, Inc.

FRANK, N. (1997): Anwendung der Thermionen-Massenspektrometrie zur Uranreihen-Datierung pleistozäner, mitteleuropäischer Travertinvorkommen. Dissertation, Universität Heidelberg.

GAAL, G., GORBATSCHEV, R. (1987): An outline of the Precambrian evolution of the Baltic Shield. Precambrian Research, 35: 15-52.

GASCOYNE, M. (1992): Geochemistry of the actinides and their daughters. In: IVANOVICH, M., HARMON, R.S.: Uranium-series disequilibrium: Applications to earth, marine and environmental sciences. Clarendon Press.

GERDES, A. (2000): Altersbestimmung und säkulare Ungleichgewichte sekundärer Kluftminerale in Graniten - eine U/Th-Isotopenstudie. Dissertation, TU Clausthal.

GOVINDARAJU, K. (1994): 1994 compilation of working values and sample description for 383 geostandards. Geostandards Newsletter 18, Special Issue: 1-158.

JOHANSSON, A. (1988): The age and geotectonic setting of the Småland-Värmland granite-porphyry belt. Geologiska Föreningens i Stockholm Förhandlingar, 110 (2): 105-110.

KAUFMAN, A., BROECKER, W. (1965): Comparison of Th^{230} and C^{14} ages for carbonate materials from lakes Lahontan and Bonneville. Journal of geophysical research, 70 (16): 4039-4054.

KEUSEN, H.R., WEIDMANN, U. (1986): Das Nagra-Felslabor Grimsel. Schweizerische Mineralogische und Petrographische Mitteilungen, 66: 492-502.

KEUSEN, H.R., GANGUIN, J., SCHULER, P., BULETTI, M. (1989): Felslabor Grimsel - Geologie. Technischer Bericht: 87-14, Nagra.

KIGOSHI, K. (1971): Alpha-recoil thorium-234: dissolution into water and the uranium-234/uranium-238 disequilibrium in nature. Science, 173: 47-48.

KORNFÄLT, K.A., PERSSON, P.O., WIKMAN, H. (1997): Granitoids from the Äspö area, southeastern Sweden - geochemical and geochronological data. Geologiska Föreningens i Stockholm Förhandlingar, 119: 109-114.

LANDSTRÖM, O., TULLBORG, E.-L. (1995): Interactions of trace elements with fracture filling minerals from Äspö Hard Rock Laboratory. Technical report: 95-13, SKB.

LANGMUIR, D. (1978): uranium solution-mineral equilibria at low temperatures with applications to sedimentary ore deposits. Geochimica et Cosmochimica Acta, 42: 547-569.

LIDE, D.R. (ed.) (1997): Handbook of chemistry and physics. CRC Press.

LOUVAT, D., MICHELOT, J.L., ARANYOSSY, J.F. (1999): Origin and residence time of salinity in the Äspö groundwater system. Applied Geochemistry, 14: 917-925.

MARSHALL, C.P., FAIRBRIDGE, R.W. (1999): Encyclopedia of geochemistry. Kluwer Academic Publishers.

MÜLLER, W.H. (1988): Felslabor Grimsel: Geologische Geschichte des Gebietes und spezielle Aspekte der Wasserführung. Nagra informiert 1+2, 13-20.

OSMOND, J.K., COWART, J.B. (1982): Natural uranium and thorium series disequilibrium: new approaches to geochemical problems. In: ZUCKER, A: Nuclear science applications. Harwood academic publishers.

RHEN, I., GUSTAFSON, G., STANFORS, R., WIKBERG, P. (1997): ÄSPÖ HRL - Geoscientific evaluation 1997/5. Models based on site characterization 1986-1995. Technical report: 97-06, SKB.

SCHALTEGGER, U. (1987): Geochemie und Rb-Sr-Systematik der Aarmassiv-Granite zwischen Grimsel und Reusstal. Schweizerischen Mineralogische und Petrographische Mitteilungen 67: 13-26

SCHEID, F. (1979): Numerische Analysis - Theorie und Anwendung. McGraw-Hill Book Company.

STANFORS, R., ERLSTRÖM, M., MARKSTRÖM, I. (1997): ÄSPÖ HRL - Geoscientific evaluation 1997/1. Overview of site characterization 1986-1995. Technical report: 97-02, SKB.

STANFORS, R., RHEN, I., TULLBORG, E.-L., WIKBERG, P. (1999): Overview of geological and hydrogeological conditions of the Äspö hard rock laboratory site. Applied Geochemistry, 14: 819-834.

STOSNACH, H. (1999): Eine Einschätzung der Verteilung von Spurenelementen in Äspö-Granitoiden und ihrer Bedeutung für die Verwendung von Graniten als geologische Barriere. Dissertation, TU Clausthal.

TRÖGER, W.E. (1967): Optische Bestimmung der gesteinsbildenden Minerale. Schweizerbartsche Verlagsbuchhandlung.

WALLIN, B., PETERMAN, Z. (1999): Calcite fracture fillings as indicators of paleohydrology at Laxemar at the Äspö Hard Rock Laboratory, Southern Sweden. Applied Geochemistry, 14: 953-962.

WEDEPOHL, K.H. (1995): The composition of the continental crust. Geochimica et Cosmochimica Acta, 59: 1217-1232.

11 Appendix: Analytical procedures

11.1 Preparation of samples

The purpose of the preparation of the HRL Äspö samples was to separate the calcite from the joint plane of the drill core completely and, if possible, without any impurities. This was achieved by means of a hand auger mounted with a ball-shaped diamond grinder (∅ 1 mm). In a further step the Äspö- as well as the Grimsel-samples were crushed in an orbital disc mill equipped with a tungsten-carbide jar and then sieved down to a grain size <63 μm.

11.2 ICP- mass spectrometry (ICP-MS)

To prepare the samples for an analysis of the trace elements by means of a mass spectrometer with inductively-coupled plasma (ICP-MS), the bulk samples were dissolved in Teflon™ autoclaves employing several acids: To some 50 to 100 mg of the sample powder 3 ml of each HNO_3 (14M), HF (23M) and $HClO_4$ (11M) were added and dissolved in a Teflon™ crucible at 180°C for 6 hours. The resulting solutions were evaporated three times to complete dryness on a hotplate, and- under the addition of 2 ml HNO_3 (14M) – refilled with deionized water to a volume of 100 ml. Furthermore, it was necessary to add to each sample solution an internal standard of rhenium, rhodium and indium (10 ppb each). Mass spectrometric analyses require calibration for each element to be measured. Five solutions were produced in each case which cover the range of expected values for the samples. For the IPC-MS measurements a quadrupole-mass spectrometer (ELAN 6000, Perkin-Elmer) was used.

The results obtained for the international reference material USGS-G2 are given in Tab. 11.1.

Tab.11.1: Accuracy of trace elements analyses by ICP-MS in the reference material G2 supplied by the United States Geological Survey.

	Li	**Rb**	**Sr**	**Y**	**Zr**	**Nb**
Average value [ppm]	28.5	172	472	8.25	310	11.0
Measured value [ppm]	34	170	478	11	309	12
Relative deviation [%]	16.2	-1.18	1.36	25.0	-0.32	8.75

	Cs	**Ba**	**La**	**Ce**	**Pr**	**Nd**
Average value [ppm]	1.30	1870	86.0	156	14.6	51.8
Measured value [ppm]	1.34	1882	89	160	18	55
Relative deviation [%]	2.99	0.66	3.43	2.28	19.2	5.82

	Sm	**Eu**	**Gd**	**Tb**	**Dv**	**Ho**
Average value [ppm]	6.85	1.39	4.10	0.43	2.15	0.36
Measured value [ppm]	7.2	1.4	4.3	0.48	2.4	0.4
Relative deviation [%]	4.86	0.71	4.65	10.4	10.4	11.3

	Er	**Tm**	**Yb**	**Lu**	**Hf**	**Ta**
Average value [ppm]	0.90	0.12	0.73	0.10	7.30	0.82
Measured value [ppm]	0.92	0.18	0.8	0.11	7.9	0.88
Relative deviation [%]	2.17	36.1	9.38	9.09	7.59	7.39

	Pb	**Th**	**U**
Average value [ppm]	27.9	25.9	2.05
Measured value [ppm]	30	24.7	2.07
Relative deviation [%]	7.17	-4.66	0.97

11.3 Isotope analyses by TIMS

Two aspects are of great importance for the analysis of the U/Th-isotopy: the separation of the U- and Th-fractions from the bulk solution, and the addition of a suitable spike. The activity of the respective isotopes (decay per minute) is taken to be a suitable unit for the interpretation of TIMS-data, which is defined on the basis of the concentration of the isotope by the following relation: Activity (A) = number of atoms (n) · decay constant (λ).

What is actually measured with the TIMS, however, is the isotope ratios, i.e. the abundance of generated ions relative to each other. The isotope concentrations can only be derived from the isotope ratios of the sample relative to those of the spike. The solutions used for the analyses presented here are a Th-spike (^{229}Th) and a uranium double-spike (^{233}U/ ^{236}U), whose exact concentrations and ^{233}U/ ^{236}U-ratios are known. These isotopes were chosen for the spike for the following reasons: they are artificially produced isotopes and thus can safely be assumed to not occur in any of the samples to be analyzed. Furthermore, their concentration practically does not change under laboratory conditions due to their long half-lives, which is important for an exact determination of the concentrations in the samples. The spike is added before the sample is processed to compensate a possible loss of uranium and thorium caused by the separation. The relations of the isotopes to one another are specified in the course of the TIMS-measurement process. If an isotope with an unknown concentration is measured simultaneously with an isotope from the spike solution, the concentration and thus the activity of the isotope can be analyzed easily.

11.3.1 Chemical preparation

Calcites

For each sample, some 100 mg of Äspö calcites and some 200 to 250 mg of Grimsel samples was dissolved in autoclaves depending on the respective uranium contents. The amount of the U- and Th-spikes had been fixed at 500 µl (Äspö samples) and 1g (Grimsel samples) respectively, an individually prepared spike was needed for the sample G 15 with an extremely high uranium concentration of 71 ppm. When the spike is added to the weighed portion, one has to take into account that nitric acid has acidified the spike and therefore reacts with the calcite, which might falsify the weight. To avoid this problem, the sample was dissolved in a sufficiently large amount of HNO_3 before spiking to drive out the CO_2. In addition to the calcite samples a blank is prepared. The dissolved samples were evaporated three times to complete dryness on a hotplate before 7M HNO_3 was added. The cooled dissolutions were filled into Teflon™ beakers, followed by re-evaporation of HNO_3 to complete dryness under infrared lamps.

The U- and Th-fractions from the bulk calcite sample were separated by means of two chromatography columns of different sizes, which were made of quartz glass and had a P2 pore frit, as described in CHEN et al. (1986). For the measurements under consideration it was sufficient to separate the U- and Th-fractions as a whole. The resin volume of the big column was 10 ml (BIORAD AG 1x8, 200-400 mesh). After a rinse with 50 ml H_2O the resin was activated by adding 50 ml HNO_3 (7 M) to the column; the concentration of the acid did not change during the entire separation run (see Fig. 11.1).

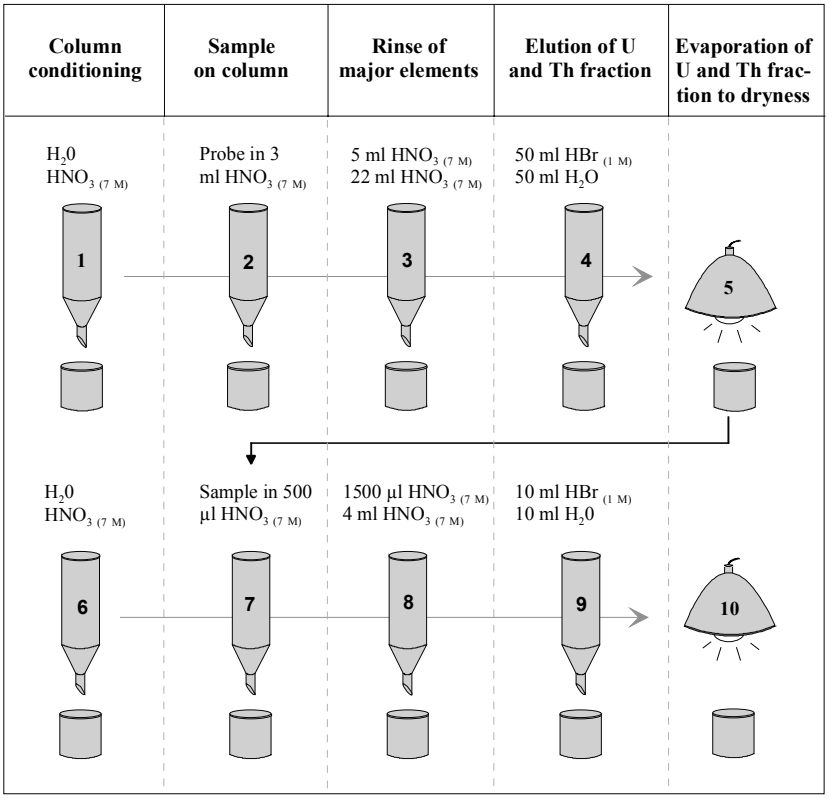

Fig. 11.1: *Flow chart for the enrichment of U and Th fractions from calcites employing ion exchange colums. For further details see text.*

- The dissolved residue was again dissolved in 3 ml and 5 ml nitric acid in two consecutive steps, and the two solutions were put on the column one after the other.

- The fraction to be discarded was separated by means of a further 22 ml HNO_3.

- After the collection beaker had been changed, 50 ml HBr (1M) was added and rinsed with 50 ml H_2O.

- The collected fraction containing U and Th was again evaporated to complete dryness under infrared lamps as a preparatory step for the separation at the small columns.

- The 2 ml column was filled with resin, rinsed with 10 ml H_2O and activated with the same amount of HNO_3.

- HNO_3 was added to the samples in increments of 500 µl and 1500 µl, which were again put on the column.

- The residual fraction was eluted with another 4 ml HNO_3, and the beaker was changed.

- Adding 10 ml HBr (1 M) and 10 ml H_2O yielded the U-Th-fraction, which was nitrified and concentrated to complete dryness again to prepare it for its application to the TIMS filament.

Silicates

The silicate samples underwent the same preparation procedures as the calcite samples. With respect to the weight of the test portion it was again the U-concentration in the individual samples which was important: for uranium contents below 1 ppm the weighed portion was 250 mg, for uranium concentrations above 1 ppm it was 100 mg. In addition to the silicates a blank was prepared, as before. The amount of the U- and Th-spikes was fixed at 1 g.

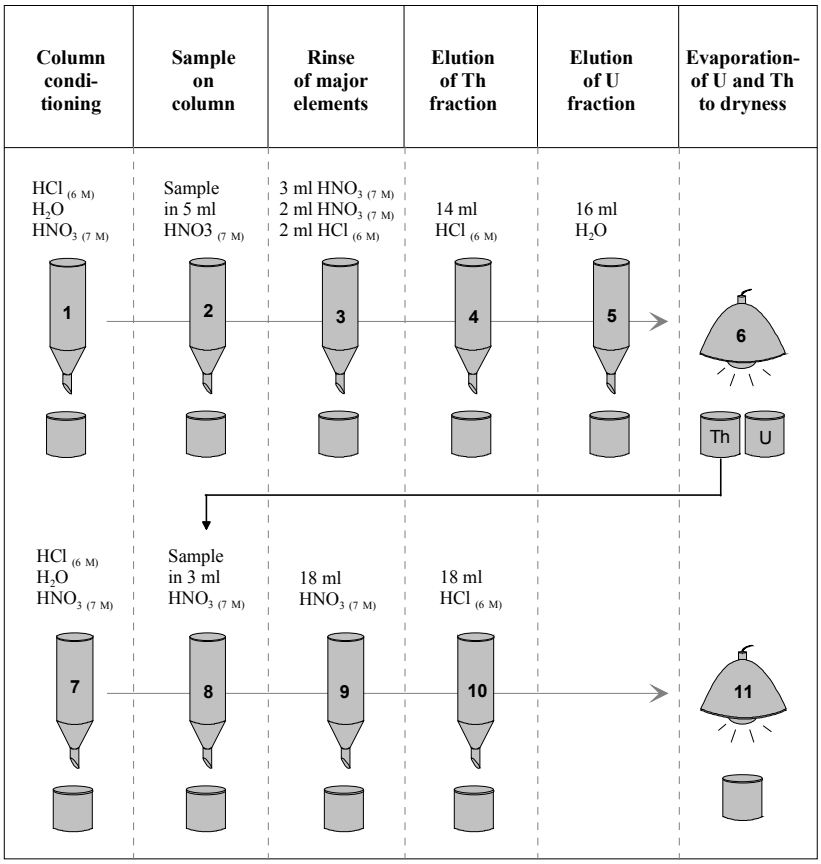

Fig. 11.2: *Flow chart for the enrichment of U and Th fractions from silicates employing ion exchange colums. For further details see text.*

In the process of separating the U- and Th-fractions from the bulk silicate samples it was crucial for the TIMS-measurement that the two elements were collected in two different fractions. This was achieved through two separation runs, both involving the small columns used in the separation process for calcites (see Fig. 11.2). The resin had a volume of 3 ml this time, but was the same as with the calcites (BIORAD AG 1x8, 200 – 400 mesh).

- Rinsing with the whole columnar volume HCl (6 M), H_2O and, finally, HNO_3 (7 M) preceded each separation run. The concentrations of the acid remained constant throughout the separation process.

- After the addition of 5 ml HNO_3 to the dissolution it was eluted with 3 ml and 2 ml of the same acid and, subsequently, with 2 ml HCl.

- With 14 ml hydrochloric acid the first Th-fraction was extracted into a new collection beaker.

- The elution of the U-fraction, for which another new beaker and 16 ml H_2O was used, followed.

- Both fractions were once more concentrated to complete dryness, the solution of the first Th-fraction was used for the second separation step.

- The Th-fraction was dissolved in 3 ml nitric acid for further purification, pipetted onto the columns filled with the conditioned resin and eluted with a further 18 ml HNO_3.

- The second, refined Th-fraction was collected in a new beaker with 18 ml HCl.

- After they have been dried again under an infrared lamp the samples are ready to be loaded on the filaments for the TIMS-measurement.

Underground solutions

The weighed portion of the solutions from the HRL Äspö was 20 ml. For the chemical preparation of the underground solutions an iron hydroxide precipitation technique was used; here the acidified sample was mixed with $FeCl_3$ and in a second step alkalinized with NH_4OH [$FeCl_3 + 3\ NH_4OH \rightarrow Fe(OH)_3\downarrow + 3\ NH_4Cl$]. For further details see CHEN et al. (1986). The resulting precipitated fraction, which also contains the U and Th resulting from this process, is again dissolved in 7 M HNO_3 and evaporated under the infrared lamp and further purified on ion exchange columns.

11.3.2 Therm-ion-mass-spectrometry (TIMS)

The basic mechanism underlying TIMS is the decomposition of the sample material into ionic and molecular elements corresponding to its specific mass, caused by thermal activation. The ions generated in this process are accelerated and then deflected depending on their charge/mass ratio in a magnetic field that acts vertically to their path. Mass spectrometers have three main components: A: ion source; B: mass separation unit; C: ion detector.

Unlike some other mass spectrometric methods, TIMS measures isotope ratios, that is the abundance of generated ions relative to each other. Concentrations can only be derived from the isotope ratios of the sample relative to a spike.

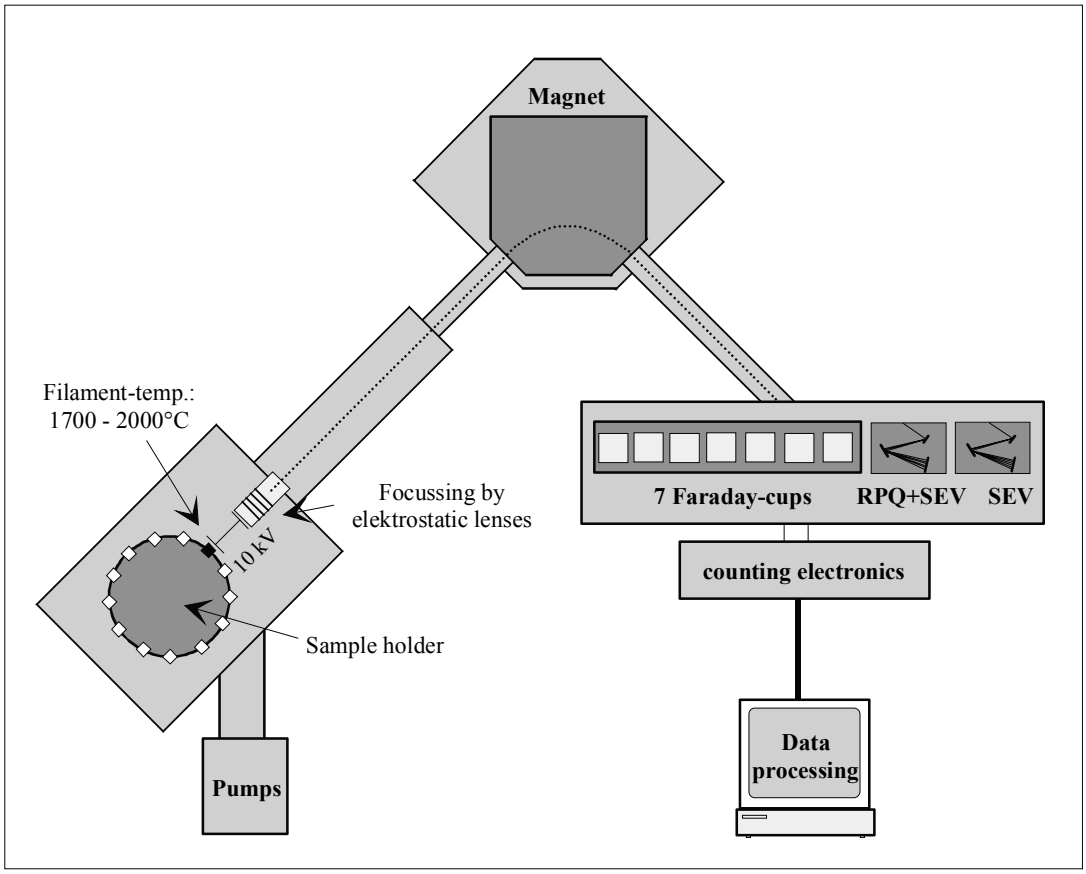

Fig. 11.3: *Components of the Therm Ion Mass Spectrometer (TIMS, MAT 262) used for U/Th isotope measurements.*

For the determination of the isotope concentrations and ratios both of the calcites from the HRL Äspö (measured at the Institute of Environmental Physics of the University of Heidelberg) and the samples from the FL Grimsel (measured at the GEOMAR Institute in Kiel) a TIMS Finnegan MAT 262 + RPQ with double filament technique was used. Fig. 11.3. shows the components of the apparatus in diagrammatic form.

Ion source: The chromatographically purified sample is loaded on the filament in nitrate form. A high vacuum is applied to the ion source as a whole (10^{-7} mbar) to avoid collisions of the accelerated ions with gas molecules. The entire system is evacuated by means of a set-up that combines a rotary pump, a turbomolecular pump, a cryopump and an ion getter pump. The filament is then electrically heated up to a temperature which is sufficient both to evaporate and to ionize the element to be analyzed. Since rhenium has a high melting point of 3180^0C, this metal is used as material for the filament. For elements with high ionization energies (e.g. uranium) the ion yield is very poor as the ionization and evaporation temperatures are different. This problem could only be countered by raising the filament temperature, which in turn would mean that the sample is used up more quickly and would thus result in poorer counting statistics. Therefore, ions are generated by means of a double filament technique in these cases. The evaporation filament loaded with the sample and an ionization filament are positioned 0.7 mm apart (FRANK 1997).

Since the evaporation temperature of thorium is higher than that of uranium, the two elements can be measured one after the other using just one filament without any noticeable loss of thorium. Ions generated in this fashion are accelerated by applying a negative voltage (10 kV), are focussed in the electrostatic lenses and directed towards the electromagnet.

Mass separation unit: One component of the TIMS mass separation unit is a 90^0 magnet with a 23 cm radius. Entering ions are deflected from their trajectory to a greater or lesser extent depending on their respective charge-mass-ratios. Assuming that the magnetic field is constant, the following relation according to FAURE (1986) is a valid approximation: $r \propto \sqrt{m}$, where r is the radius of the trajectory and m the mass of the isotope under analysis. It follows that ions with a greater mass are forced onto trajectories with radii greater than those of the trajectories of light ions, which are less strongly affected by the magnetic field. There are three possible methods to carry out the measurement:

1. The accelerating voltage can be varied, keeping the magnetic field strength constant ('peak-jumping mode' based on a variable voltage).
2. The magnetic field strength can be varied, keeping the accelerating voltage constant ('peak-jumping mode' based on a variable magnetic field strength).
3. Both the accelerating voltage and the strength of the magnetic field are kept constant so that different detectors are needed for the radii in question (static measuring mode).

Ion detector: An additional feature of the TIMS described here is a multicollector system with two different detector types which are applied depending on the intensity of the input signal. For ionic currents > 10^{-5} seven Faraday-cups, some of them movable, are used. For weaker signals this device uses secondary electron multipliers (SEM). Up to seven masses can be detected simultaneously with this cup line-up. Each ion charge of a given mass is collected in one of the Faraday-cups equipped with a high-ohmic resistor (10^{11} Ω). The voltage generated at the resistance is proportional to the strength of the ionic current. In a further step it is increased and finally converted into a digital signal. In addition, an RPQ-system ('Retarding Potential-Quadrupole'), which includes a focusing device and a static quadrupol, and a secondary electron multiplier can be connected in series. Ions which deviate from the trajectory determined exactly for a given mass are filtered out of the ion beam and discarded.